

3.1 Introduction

Twice a year, at the time of the equinoxes, westerly winds abruptly start to blow over the central Indian Ocean. The response of the ocean is dramatic and curious. An intense narrow eastward jet, with speeds comparable to that of the Gulf Stream, appears in the surface layers of the ocean within weeks after the onset of the winds (Wyrтки, 1973b). The jet is only a few hundred kilometers wide and clearly marks the location of the equator even though there is nothing exceptional about the structure of the winds in the neighborhood of the equator. At first the jet accelerates—during October 1973 as shown in Fig. 3.1, for example—but this acceleration stops abruptly after a few weeks, although the winds continue to provide eastward momentum to the ocean. Subsequently the jet decelerates and reverses direction. The winds, however, never reverse direction. The trajectories of buoys that drifted in the current in late 1979 indicate that the reversal of the jet first occurred in the east near Sumatra. In Fig. 3.2, buoy 1804 is seen to start traveling westward at a time when buoys 1090 and 1803 farther to the west are still traveling eastward at a high speed. The latter two buoys start to drift westward at points increasingly farther from the coast of Sumatra. It is as if a signal propagating westward at an approximate speed of 55 cm/sec caused the buoys to reverse direction. Presumably the arrival of this signal at Gan (Fig. 3.1) causes the deceleration of the jet observed there.

The events described raise a number of questions. Why does a jet appear at the equator and what determines its width? What causes it to accelerate initially and to reverse direction subsequently? Why does the reversal start

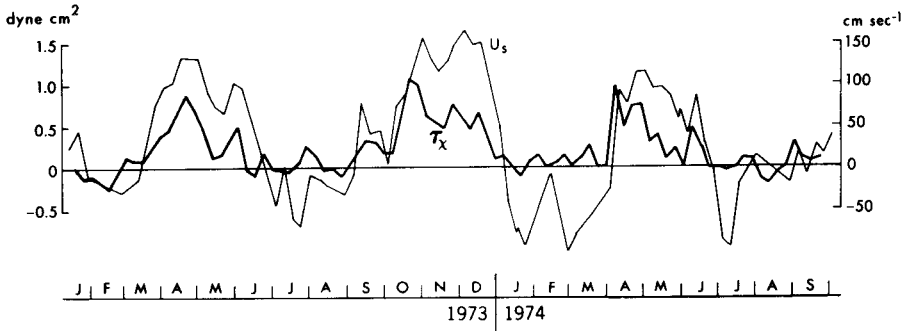


Figure 3.1. The zonal velocity component at the surface and the zonal component of the windstress, as measured in the central Indian Ocean on the equator near Gan (70°E). [From Knox (1976).]

in the east? How long would it have taken the ocean to reach a state of equilibrium had the winds remained constant after their sudden onset? In other words, how long is the “memory” of the ocean?

Examples of the rapid response of tropical oceans to large-scale changes in the surface winds are numerous. Chapter 2 describes basinwide seasonal and interannual changes in the circulations of each of the three tropical oceans. In the subtropics and midlatitudes, on the other hand, comparable variability involving the Gulf Stream and Antarctic Circumpolar Current, for example, appears only on far longer time scales. This suggests that the time it takes the ocean to adjust to a change in the winds increases with increasing latitude. The memory of the ocean is far longer in high than in low latitudes. What physical processes determine the memory?

The measurements in Figs. 3.1 and 3.2 describe variations in the Indian Ocean but an understanding of these variations can shed light on a host of other phenomena, including El Niño. It is important to know how long the memory of the ocean is because it is this memory that presumably permits anomalous oceanic and atmospheric conditions associated with the Southern Oscillation to persist for several seasons. (The time it takes the atmosphere to return to a state of radiative equilibrium after a change in its heating is of the order of a month, far shorter than the time scale of the Southern Oscillation.) Of interest is how long it takes the ocean to reach a state of dynamic equilibrium. For example, how long would it take the ocean to become motionless should the winds suddenly stop blowing? In the final state of rest there are no horizontal density gradients but there can be vertical gradients. The time to establish the vertical gradients, the stratification of the ocean, is believed to be of the order of decades. This is much longer than the time for the changes in the oceanic circulation

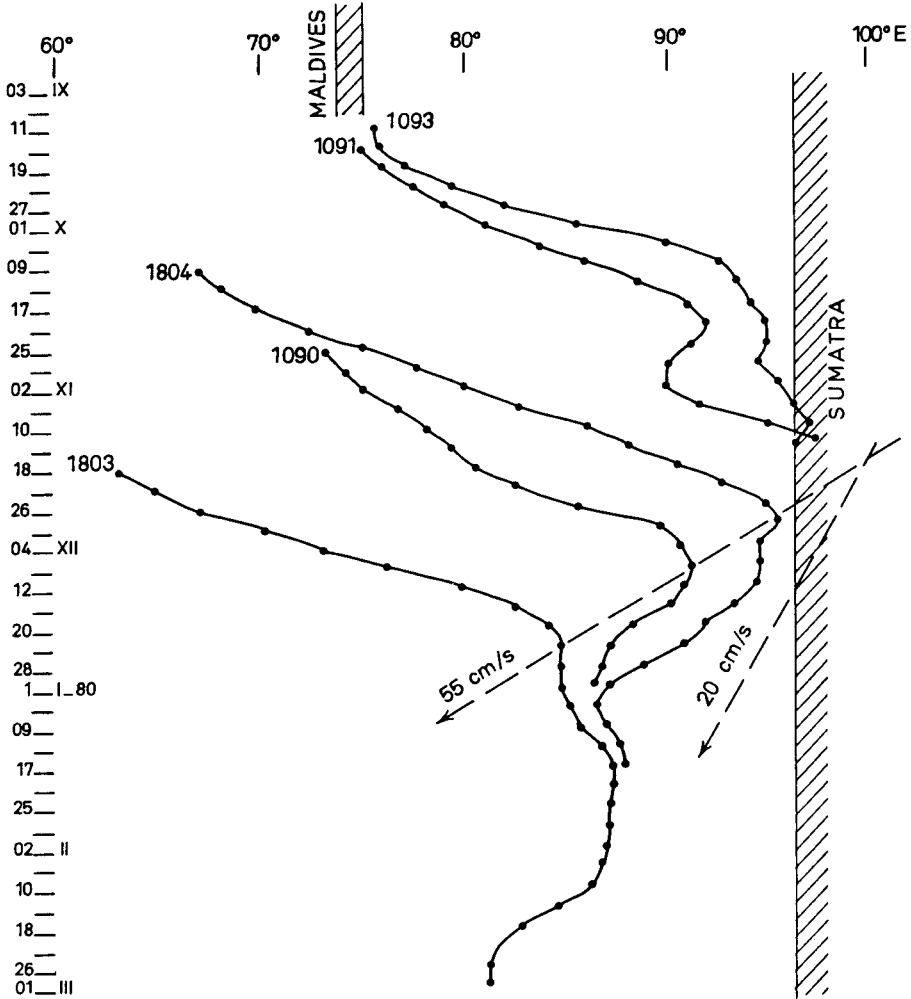


Figure 3.2. The movement of buoys that drifted with the surface currents along the equator in the Indian Ocean between 3 September 1979 and 1 March 1980. The first two buoys washed ashore on Sumatra. [From Gonella *et al.* (1981).]

between El Niño and La Niña. In studies of the oceanic adjustment it is therefore assumed that the vertical stratification of the ocean is given—the processes that maintain the thermocline are not considered—and attention is focused on the manner in which the winds generate horizontal density gradients and currents on the relatively short time scale of the Southern Oscillation.

3.2 The Shallow-Water Model

An appealingly simple model of the tropical oceans can provide answers to the questions raised by Figs. 3.1 and 3.2. In the model, the interface between two immiscible layers of fluid, each of constant density, simulates the sharp and shallow tropical thermocline that separates the warm surface waters from the cold waters of the deep ocean. The upper layer has density ρ_1 , has a mean depth H , and is bounded above by a rigid lid. The lower layer has density ρ_2 and is infinitely deep so that it must be motionless for the kinetic energy to be finite. (In reality the ocean is 4000 m deep and the thermocline is at a depth of approximately 100 m.) Linear hydrostatic motion in the upper layer is driven by the windstress τ that acts as a body force. This motion is associated with a displacement η of the interface and is described by the shallow-water equations¹

$$u_t - fv + g'\eta_x = \tau^x/H \quad (3.1a)$$

$$v_t + fu + g'\eta_y = \tau^y/H \quad (3.1b)$$

$$g'\eta_t + c^2(u_x + v_y) = 0 \quad (3.1c)$$

The Cartesian coordinate system, which is fixed in the rotating earth, is shown in Fig. 3.3. The velocity components in the eastward (x) and northward (y) directions are u and v , respectively, while t measures time. The equator is at $y = 0$. Effects caused by the rotation and curvature of the earth enter through the Coriolis parameter

$$f = \beta y, \quad \text{where } \beta = 2\Omega/a \quad (3.2)$$

Here Ω denotes the rate of rotation of the earth and a its radius. The gravitational acceleration g , because of the stratification, is effectively reduced to

$$g' = \frac{\rho_2 - \rho_1}{\rho_1} g \quad (3.3)$$

The gravity wave speed is

$$c = (g'H)^{1/2} \quad (3.4)$$

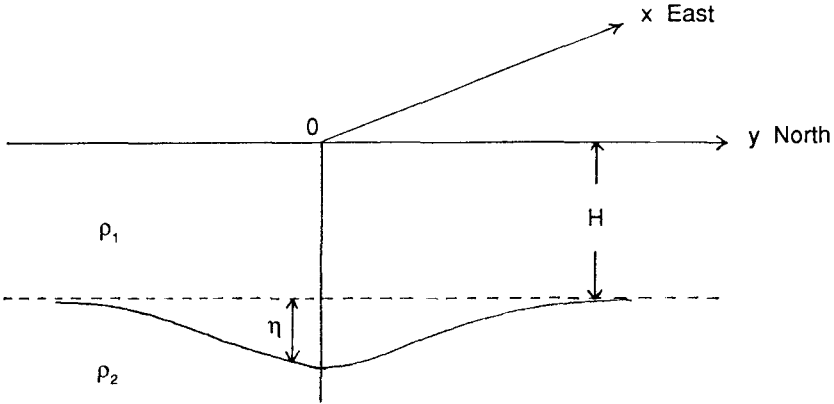


Figure 3.3. The Cartesian coordinate system.

This is sometimes written

$$c = (gh)^{1/2} \quad (3.5)$$

where h is known as the equivalent depth. Reasonable numerical values are

$$\frac{\rho_2 - \rho_1}{\rho_1} = 0.002; \quad H = 100 \text{ m}; \quad h = 20 \text{ cm}; \quad c = 1.4 \text{ m/sec} \quad (3.6)$$

Equations (3.1) can be reduced to a single equation for the northward velocity component v :

$$(v_{xx} + v_{yy})_t + \beta v_x - c^{-2} v_{tt} - \frac{f^2}{c^2} v_t = F \quad (3.7)$$

where

$$F = \frac{f^2}{c^2} \left(\frac{\tau^x}{H} \right)_t - \frac{1}{c^2} \left(\frac{\tau^y}{H} \right)_{tt} + \frac{1}{H} \frac{\partial}{\partial x} \left(\frac{\partial \tau^x}{\partial y} - \frac{\partial \tau^y}{\partial x} \right)$$

In regions that are far from the equator and that have a latitudinal extent L sufficiently small for the Coriolis parameter to be regarded as a constant (even though its y derivative, β , is also regarded as a nonzero constant), the vorticity equation (3.7) can be simplified provided the following conditions are satisfied: the time scale under consideration must be much longer than the local inertial period and the rotational Froude number of the motion (fL/c) must be at most order one. Under these conditions, Eq. (3.7) can be

written in terms of a stream function such that $v = \psi_x$ and $u = -\psi_y$:

$$\left(\psi_{xx} + \psi_{yy} - \frac{f^2}{c^2} \psi \right)_t + \beta \psi_x = \text{curl}_z \tau \quad (3.8)$$

A steady solution to the original equations (3.1) can readily be written down without invoking the approximations that lead to Eq. (3.8):

$$\beta v = \text{curl}_z \tau \quad (3.9)$$

This equation was first used by Sverdrup (1947) to explain how the curl of the wind drives the surface currents in Fig. 2.1. If the curl of the wind is zero then the solution to Eqs. (3.1) is

$$u = v = 0, \quad g' \eta_x = \tau^x / H \quad (3.10)$$

This solution, and hence the inviscid model, appears unpromising at first because it predicts that steady, uniform, zonal winds maintain a pressure gradient but do not drive any currents. The model nonetheless deserves attention for its description of the evolution of equilibrium conditions after the sudden onset of the winds. To put it another way, the journey is more important than the destination. An understanding of the fascinating transients that appear before equilibrium is attained greatly facilitates the interpretation of results from more realistic and complex models.

3.3 The Equatorial Jet

Consider the motion induced by the sudden onset of spatially uniform zonal winds that then remain steady. Initially the flow in the interior of the ocean basin, far from coasts, is independent of longitude. Zonal variations become important when the effects of coasts penetrate to the interior of the basin, but until such time set $\partial/\partial x = 0$ in Eq. (3.7):

$$v_{tt} + f^2 v - c^2 v_{yy} = -f \tau^x / H \quad (3.11)$$

At large distances L from the equator, and after a time longer than the local inertial period $2\pi/\beta L$, the second term dominates the left-hand side of this equation so that

$$v = -\tau^x / fH \quad (3.12)$$

This expression for the Ekman drift, which is to the right of the wind in the Northern Hemisphere and to the left in the Southern Hemisphere, is valid provided the distance L from the equator exceeds the local value of the radius of deformation λ^* , where

$$\lambda^* = c/f \quad (3.13)$$

The Ekman drift, which converges on the equator if the winds are eastward, amplifies with decreasing latitude so that downwelling must be intense near the equator. Not only the vertical component of the velocity but also the zonal component is strong because Eq. (3.1a) implies that, in the absence of zonal gradients, the wind accelerates the ocean steadily: $u_t = \tau^x/H$ at $y = 0$. A distinctive equatorial zone clearly exists. Its width can be inferred from a scale analysis of (3.11) and is the distance from the equator where the second and third terms on the left-hand side of this equation have comparable magnitudes. This distance

$$\lambda = (c/\beta)^{1/2} \sim 250 \text{ km} \quad (3.14)$$

is known as the equatorial radius of deformation. The time scale

$$T = (\beta c)^{-1/2} \sim 1.5 \text{ days} \quad (3.15)$$

which determines the relative importance of the first two terms in Eq. (3.11), is the inertial time $1/f$ at the latitude λ . Shortly after the winds start to blow ($0 < t \ll T$) the first term in (3.11) is far larger than the second term, which represents rotational effects. During this period there is nothing distinctive about the neighborhood of the equator because the rotation of the earth is unimportant. It follows that T is the time it takes for a distinctive equatorial zone to form.

Next confine attention to times much longer than T so that the first term in Eq. (3.11) is negligible. Physically, this approximation filters out high frequency inertia-gravity waves that are excited by the sudden onset of the winds. The solution to Eq. (3.11) can then be written as (Yoshida, 1959)

$$v = -\frac{\tau^x}{H}(\beta c)^{-1/2}Q \quad (3.16a)$$

$$u = \frac{\tau^x}{H}t(1 - \xi Q) \quad (3.16b)$$

$$\eta = -\tau^x \frac{t}{c} Q_\xi \quad (3.16c)$$

where

$$\eta = y/\lambda$$

The function Q , the velocity components, and the interface displacements are shown in Fig. 3.4. The solution describes an accelerating equatorial jet whose half-width is twice the radius of deformation, approximately 500 km. The meridional Ekman drift is steady and is maintained by a steady deepening of the thermocline near the equator. The associated increase in the latitudinal density gradient is such that the accelerating equatorial jet is

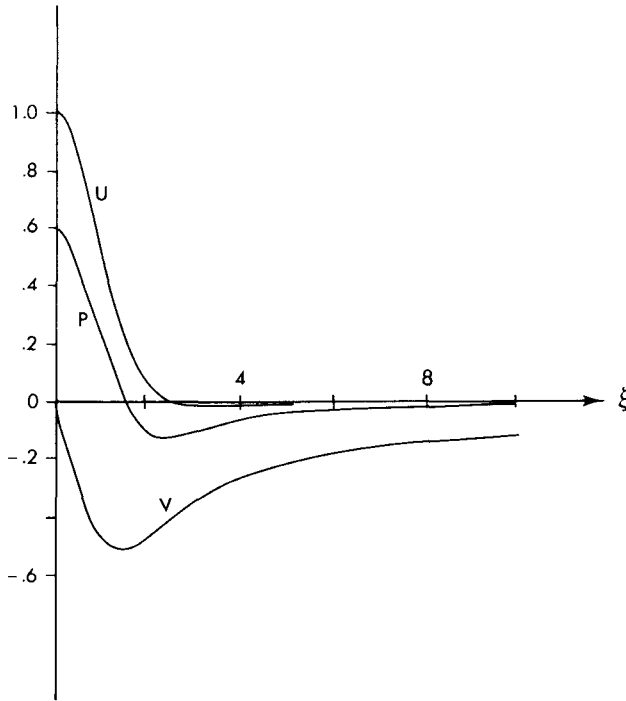


Figure 3.4. The latitudinal structure of the accelerating equatorial jet (U), of the steady meridional flow (V), and of the thermocline displacement (P) in response to spatially uniform eastward winds. The unit for latitude is the equatorial radius of deformation. [From Moore and Philander (1977).]

always in geostrophic balance:

$$fu + g'\eta_y = 0 \quad (3.17)$$

Geostrophic motion is a form of resonance because it persists in the absence of any forcing. Hence, if the winds should suddenly stop blowing after a time t_0 , then the acceleration of the jet, the equatorward Ekman drift, and the deepening of the equatorial thermocline will all stop, while a steady geostrophic equatorial jet of intensity $u = \tau^x t_0 / H$ at $y = 0$ will persist indefinitely in the absence of dissipation and meridional coasts. Under these conditions the ocean has a memory and records how long the winds had blown. To destroy the equatorial jet generated by winds that had blown eastward for a certain time, it is necessary to blow winds westward for exactly the same time.

Accelerating jets eventually become nonlinear and unstable, but the next complication to account for is the effect of meridional coasts at $x = 0$ and

$x = L$. At these walls the zonal flow u must vanish at all times. This can be accomplished by superimposing on the wind-driven jet just described the free modes of oscillation of the ocean. These are discussed in the next section.

3.4 Waves

The model described by Eqs. (3.1) permits two types of waves: inertia-gravity waves, which have restoring forces owing to the stratification of the ocean and the rotation of the earth, and Rossby waves, which have restoring forces owing to the latitudinal variation of the Coriolis parameter. Consider waves with zonal wavelength $2\pi/k$ and frequency σ :

$$v = V(y)\exp(ikx - i\sigma t) \quad (3.18)$$

Adopt the convention that σ is always positive so that the sign of k determines the direction of zonal phase propagation. (Phase propagation is eastward if $k > 0$ and westward if $k < 0$.) Substitution of (3.18) into (3.8) gives

$$V_{yy} + \frac{\beta^2}{c^2}(Y^2 - y^2)V = 0 \quad (3.19)$$

where

$$Y^2 = \left(\frac{\sigma^2}{c^2} - k^2 - \frac{\beta k}{\sigma} \right) \frac{c^2}{\beta^2}$$

Solutions to Eq. (3.19) are wavelike (oscillatory) in an equatorial zone of width $2Y$ but are exponentially decaying poleward of latitudes $\pm Y$. These latitudes depend on the wave number and frequency of the wave and have a maximum value when

$$k = -\beta/2\sigma \quad (3.20)$$

in which case

$$Y^2 = Y_{\max}^2 = \frac{\sigma^2}{\beta^2} + \frac{c^2}{4\sigma^2} \quad (3.21)$$

In Fig. 3.5, which shows Y_{\max} as a function of frequency, the width of the equatorial waveguide has a minimum value at the frequency

$$\sigma = (\beta c/2)^{1/2} \quad (3.22)$$

In extraequatorial latitudes no waves are possible in a band of frequencies centered on this value. The approximate limits of the band, which separates

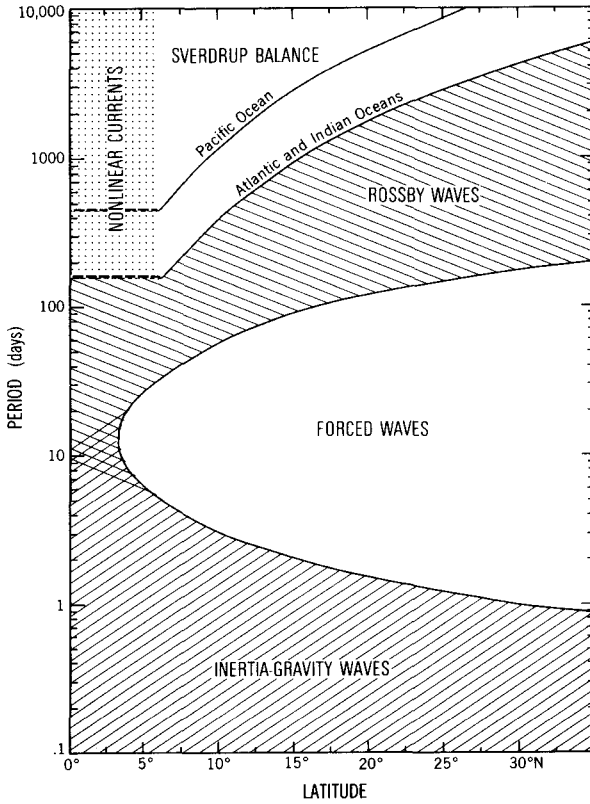


Figure 3.5. Periods, as a function of latitude, at which fluctuating winds excite oceanic inertia-gravity, Rossby, and no free waves—in other words, only forced waves. At very long periods, which depend on the zonal extent of the basin, the response to variable winds is an equilibrium Sverdrup balance. The Indian and Atlantic Oceans are assumed to be 5000 km wide and the Pacific 15,000 km wide.

high-frequency inertia-gravity waves from low-frequency Rossby waves, can be obtained by assuming that the waves far from the equator have such short meridional wavelengths that the value of the Coriolis parameter is practically constant over several wavelengths. Locally the latitudinal dependence of V can then be written $\exp(iny)$. A dispersion relation follows from (3.19):

$$\sigma^2 = f_0^2 + gH(k^2 + n^2 + \beta k/\sigma) \tag{3.23}$$

At high frequencies this expression simplifies to

$$\sigma^2 = f_0^2 + gH(k^2 + n^2) \tag{3.24}$$

which is a dispersion relation for inertia-gravity waves. Their frequency always exceeds the local inertial frequency f_0 .

At low frequencies $\sigma \ll f_0$,

$$\sigma = -\beta k / (k^2 + n^2 + f_0^2/c^2) \quad (3.25)$$

The frequency σ is by definition positive so that the zonal wave number k must have a negative value. In other words, all Rossby waves have westward phase propagation. A further restriction on the wave number can be inferred from (3.25):

$$k^2 + \beta k / \sigma < 0 \quad (3.26)$$

This means that Rossby waves are excited in the ocean only if the Fourier components of the forcing function have wave numbers and frequencies that satisfy this condition. The dispersion diagram for Rossby waves shows that although the waves have westward phase speed, their zonal group velocity can be either eastward (for waves with a zonal scale smaller than the radius of deformation λ^*) or westward (for long waves with a horizontal scale that exceeds λ^*) (Fig. 3.6). Waves with zero group velocity have the highest possible frequency

$$\sigma_{\max}^2 = \beta c / 2f_0 \quad (3.27)$$

This relation gives the maximum value that the Coriolis parameter can have for waves with frequency σ . In other words, Rossby waves can propagate only equatorward of the latitude where the Coriolis parameter has the value given by Eq. (3.27). The very long waves are nondispersive, have a zonal velocity component that is in approximate geostrophic balance, and have a

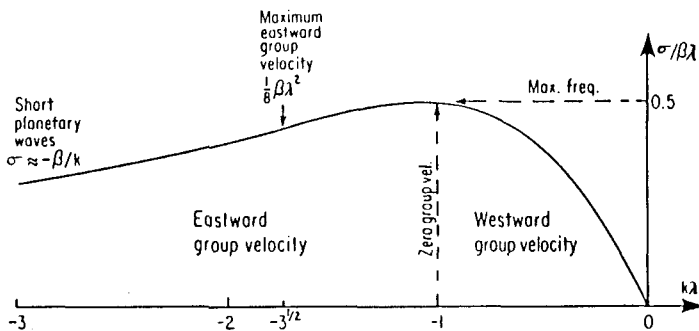


Figure 3.6. A dispersion diagram for Rossby waves that can be written as $\sigma/\beta\lambda = -k\lambda/(1 + (k\lambda)^2)$, where σ is frequency and $\lambda = c/f$ is the radius of deformation. [From Gill (1985).]

speed

$$s = -\beta c^2/f_0^2 \quad (3.28)$$

The short waves, with eastward group velocities, are much slower than the long waves—their maximum group velocity is $s/8$ —and are prone to dissipation. These short waves are relatively unimportant in the oceanic adjustment to a change in wind conditions, but the long nondispersive waves are of paramount importance in the adjustment. The long waves reflect off the western boundaries of ocean basins as short Rossby waves that do not propagate far offshore before being dissipated, so that energy tends to accumulate close to western boundaries. The zonal asymmetry of Rossby wave dispersion is of great importance in a number of phenomena to be studied later.

3.4.1 Ray Paths

Consider a packet of Rossby waves with a latitudinal scale sufficiently small for the Coriolis parameter f to be regarded as a local constant. As the packet propagates over a large latitudinal distance, the value of f changes so that the dispersion relation (3.25) can be regarded as a slowly varying function of latitude y . This implies that the group velocity vector of the packet changes gradually with latitude. This vector is the tangent to the ray path so that

$$\frac{dx}{dy} = \frac{\partial \sigma}{\partial n} / \frac{\partial \sigma}{\partial k} = -\frac{2\sigma}{\beta} \left(-\frac{\beta k}{\sigma} - \frac{\beta^2 y^2}{c^2} \right)^{1/2} \quad (3.29)$$

The coordinates of the ray path are (x, y) , and the dispersion relation (3.25) has been simplified by confining attention to long Rossby waves ($k^2 \gg f^2/c^2$). From (3.29) it follows that

$$y = \left(-\frac{c^2 k}{\sigma \beta} \right)^{1/2} \cos \left(\frac{2\sigma}{c} x + \theta_0 \right) \quad (3.30)$$

The constant of integration is θ_0 . Figure 3.7 shows these rays for waves that emanate from the eastern boundary of the basin with a period of 0.5 year and with an initial meridional wave number that is zero. (The value of the meridional wave number changes along the path but the zonal wave number and frequency remain unchanged.) Figure 3.7 shows the equatorward refraction of the wave packet because of the latitudinal variation of the Coriolis parameter. This refraction can result in waves that are equatorially trapped.

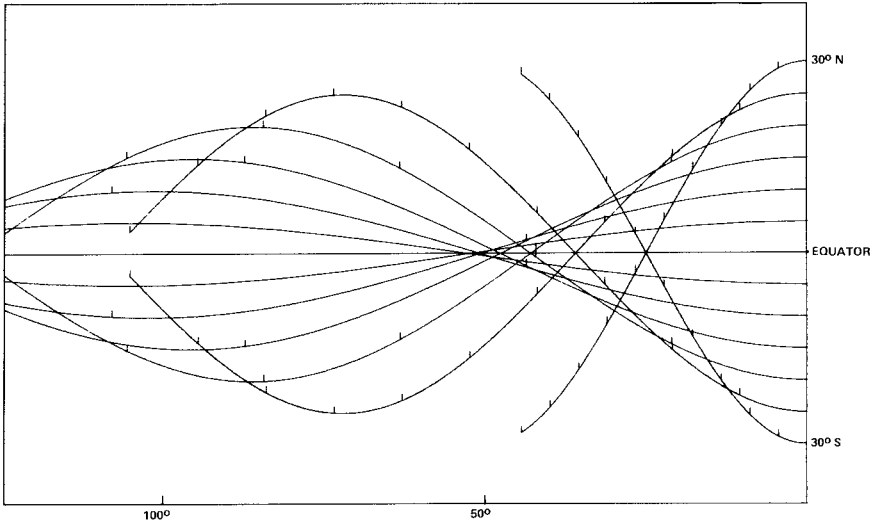


Figure 3.7. Ray paths for Rossby waves with a period of one year that start at the eastern boundary of the ocean basin with a meridional wave number equal to zero. [From Schopf *et al.* (1981).]

The rays in Fig. 3.7 seem to be refracted towards a focal point (caustic) on the equator approximately 50° in longitude from the eastern coast. From Eq. (3.30) it follows that this distance is given by

$$x = (2r + 1)\pi c/4\sigma, \quad r = 0, 1, 2, \dots \quad (3.31)$$

(The constant θ_0 is zero for the case under consideration.) After passing through a focus the waves propagate poleward as far as their turning latitude and are then refracted towards another caustic on the equator. These results explain features of certain models but are of limited relevance to the ocean because of the neglect of mean currents.

3.4.2 Equatorially Trapped Waves

The superposition of a wave that propagates towards its northern turning latitude and another wave with the same frequency and wave number that propagates to the south could result in a standing latitudinal mode. Such modes, which span the equator and which are evanescent poleward of the turning latitude, are known as equatorially trapped modes.² An arbitrary superposition of waves traveling in opposite directions will in general not result in standing modes. Modes are possible only for certain discrete values of the meridional wave number n that are eigenvalues of Eq. (3.19) subject to the condition that solutions are bounded at large values of $|y|$. These

eigenvalues are given by the expression

$$\frac{c}{\beta} \left(\frac{\sigma^2}{c^2} - k^2 - \frac{\beta k}{\sigma} \right) = 2n + 1, \quad n = 0, 1, 2, \dots \quad (3.32)$$

This is the dispersion relation for equatorially trapped modes whose latitudinal structure is described by the eigenfunctions of (3.19):

$$V = D_n(y/\lambda) \quad (3.33)$$

The D_n are Hermite functions of order n ,

$$D_n = e^{-\xi^2/2} H_n(\xi), \quad \xi = y/\lambda \quad (3.34)$$

where H_n is the n th Hermite polynomial.³ The functions are orthogonal so that

$$\int_{-\infty}^{\infty} D_m D_n d\xi = 2^n n! \pi^{1/2} \delta_{mn} \quad (3.35)$$

where

$$\delta_{mn} = 1, \text{ if } m = n \quad \text{and} \quad \delta_{mn} = 0, \text{ if } m \neq n$$

The zonal velocity component and pressure are given by the expressions

$$\begin{aligned} u &= i(2\beta)^{1/2} \exp(ikx - i\sigma t) \left[\frac{n^{1/2} D_{n-1}}{\sigma + ck} + \frac{(n+1)^{1/2} D_{n+1}}{\sigma - ck} \right] \\ \eta &= -(2\beta)^{1/2} \exp(ikx - i\sigma t) \left[\frac{n^{1/2} D_{n-1}}{\sigma + ck} - \frac{(n+1)^{1/2} D_{n+1}}{\sigma - ck} \right] \end{aligned} \quad (3.36)$$

For an equatorial wave mode with amplitude A the energy density is

$$\begin{aligned} E &= \frac{1}{2} \int_{-\infty}^{\infty} \overline{(u^2 + v^2 + c^2 \eta^2 / H^2)} dy \\ &= \frac{1}{4} A^2 \left[1 + \frac{n+1}{(\sigma - ck)^2} + \frac{n}{(\sigma + ck)^2} \right] \end{aligned} \quad (3.37)$$

and the zonal energy flux is

$$\begin{aligned} F &= g' \int_{-\infty}^{\infty} \overline{\eta u} dy \\ &= \frac{1}{4} A^2 \left[\frac{n+1}{(\sigma - ck)^2} - \frac{n}{(\sigma + ck)^2} \right] \end{aligned} \quad (3.38)$$

The overbar denotes a time average. Since

$$F = E c_g$$

the energy equation, which is derivable from Eqs. (3.1) in the absence of forcing, can be written

$$E_t + c_g E_x = 0 \quad (3.39)$$

The group velocity $c_g (= \partial\sigma/\partial k)$ can be calculated from the dispersion relation (3.32). Equation (3.32) gives two curves for each value of n : one for inertia-gravity waves and the other for Rossby waves, as shown in Fig. 3.8. The odd modes ($n = 1, 3, 5, \dots$) are symmetrical about the equator and the even modes are antisymmetrical. Figure 3.9 depicts their structure. Since n

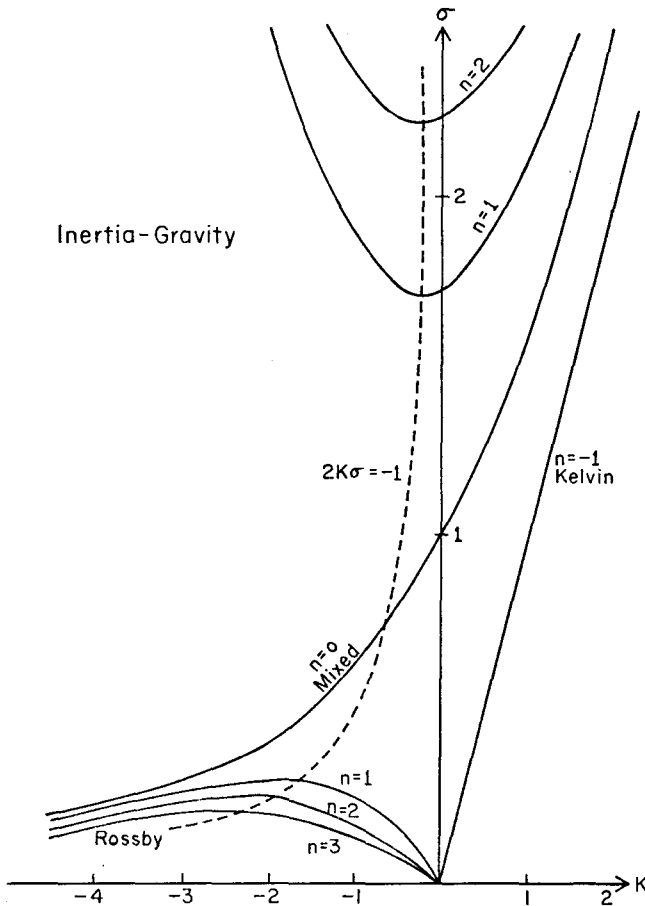


Figure 3.8. Dispersion diagram for equatorially trapped modes. The unit of frequency is $(\beta c)^{1/2}$ and the unit of zonal wave number k is the inverse of the radius of deformation $(c/\beta)^{1/2}$. [From Cane and Sarachik (1976).]

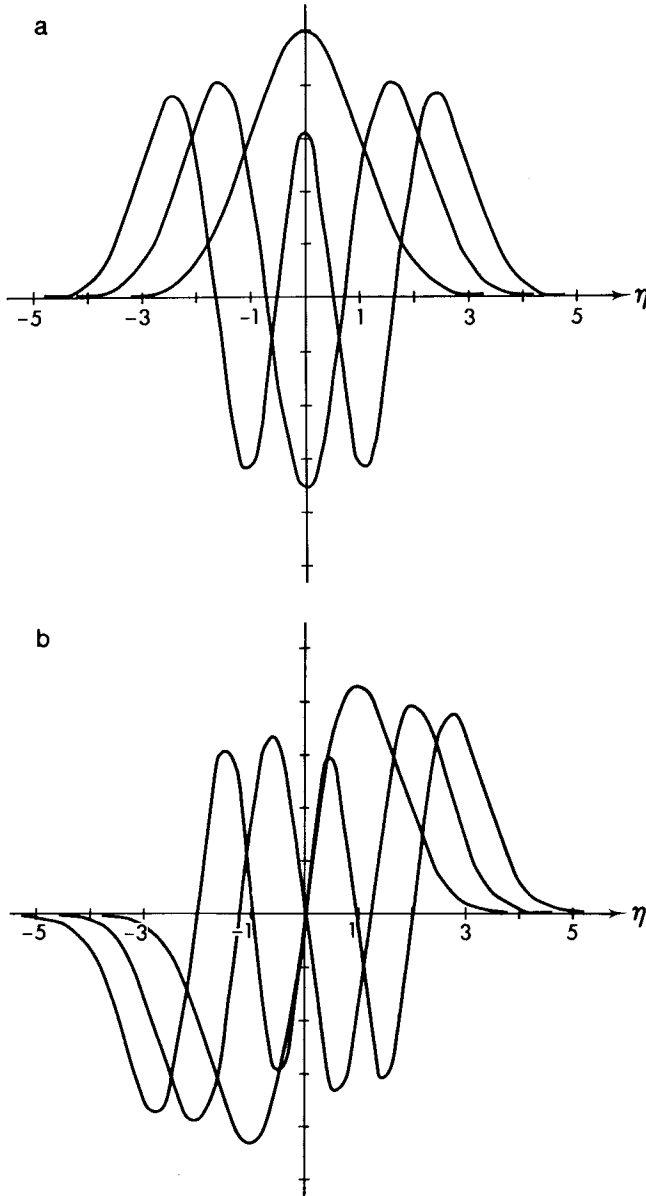


Figure 3.9. The latitudinal structure of (a) symmetrical and (b) antisymmetrical Hermite functions that describe the meridional velocity component. The unit of distance in the northward direction is the equatorial radius of deformation.

corresponds to the number of zeroes that a mode has, it can be regarded as a meridional wave number. As n increases, the turning latitude increases. For large values of n the Hermite functions are essentially sinusoidal except in the neighborhood of and poleward of their turning latitudes. For $n \gg 1$ the dispersion relation (3.23) is a good approximation to (3.32).

The gravest equatorially trapped mode deserves special comment. According to Eq. (3.32) there are two roots for $n = 0$:

$$\begin{aligned} k &= -\sigma/c \\ k &= \sigma c - \beta/c \end{aligned} \quad (3.40)$$

The first root must be discarded because the associated u and η grow exponentially for large values of y even though v is bounded. The other root is known as the Rossby-gravity mode (see Note 2) because it is similar to inertia-gravity waves at high frequencies and similar to Rossby waves at low frequencies. The latitudinal shape of the meridional velocity component is a Gaussian centered on the equator; the zonal flow is antisymmetrical about the equator. Weisberg *et al.* (1979) describe measurements that are consistent with the structure of this wave.

At low frequencies the dispersion relation (3.32) simplifies to

$$\sigma = \frac{-\beta k}{k^2 + \frac{2n+1}{\lambda^2}}, \quad n = 1, 2, 3, \dots \quad (3.41)$$

from which it follows that equatorially trapped Rossby waves are very similar to the Rossby waves discussed earlier: the slow, short, dispersive waves have eastward group velocities and the fast, long, nondispersive waves have westward group velocities $c/(2n+1)$. The most rapid Rossby wave ($n = 1$) travels at one-third the speed of long gravity waves. Its structure is shown in Fig. 3.10. The zonal current has a maximum and the thermocline displacement a minimum on the equator.

The long Rossby waves are of paramount importance in the oceanic adjustment to a change in the winds. The inertia-gravity, Rossby-gravity, and short Rossby waves are relatively unimportant and can be filtered from the equations of motion by making the “long wave” approximations. It is necessary that the scale of zonal variations, L , be much larger than the radius of deformation λ . The scale of latitudinal variations can, however, be comparable to λ . It is also necessary that the magnitude of the zonal flow exceed that of the meridional flow by a factor of L/λ at least. This assumption is justified by measurements at the equator that consistently show that at low frequencies—periods longer than a month—zonal velocity fluctuations are far more energetic than meridional velocity fluctuations

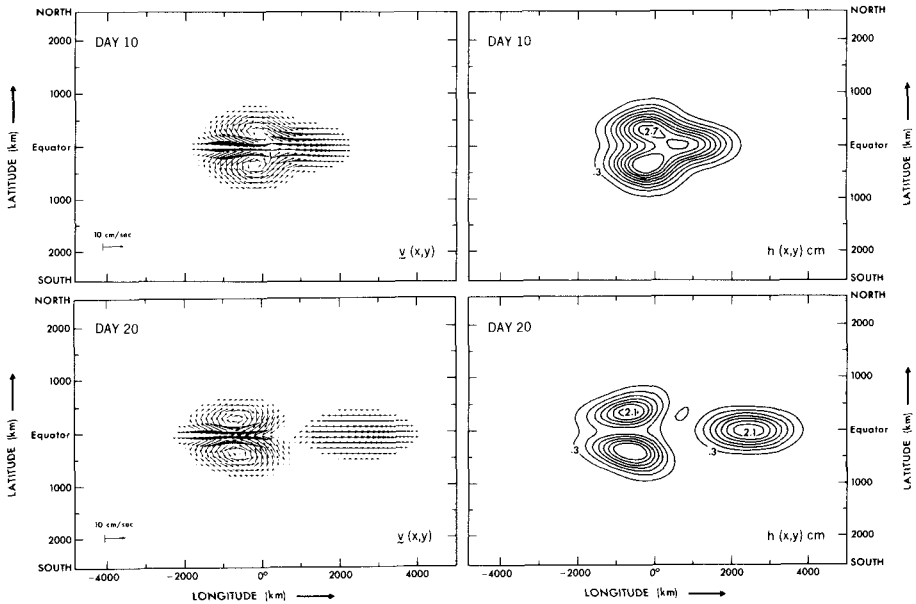


Figure 3.10. The dispersion of an initially bell-shaped thermocline displacement into an eastward-propagating Kelvin wave and westward-propagating Rossby waves. The left-hand panels show the horizontal currents and the right-hand panels the thermocline displacements. [From Philander *et al.* (1984).]

(Knox and Anderson, 1985). Under these conditions the shallow-water equations simplify to

$$\begin{aligned} u_t - fv + g'\eta_x &= 0 \\ fu + g'\eta_y &= 0 \\ g'\eta_t + c^2(u_x + v_y) &= 0 \end{aligned} \quad (3.42)$$

These equations yield a vorticity equation

$$\left(v_{yy} - \frac{f^2}{c^2} v \right)_t + \beta v_x = 0 \quad (3.43)$$

so that

$$v = F\left(x + \frac{c}{2n+1}t\right) D_n(y) \quad (3.44)$$

where F is an arbitrary function and D_n is a Hermite function. These long Rossby waves have their zonal flow in geostrophic balance.

To isolate short, low-frequency Rossby waves, which are important primarily in the neighborhood of the western boundaries of ocean basins, it is necessary to assume that the zonal wave number is large ($k \gg 1/\lambda$) and that the frequency is low [$\sigma \ll (\beta c)^{1/2}$]. The equations of motion then simplify to

$$\begin{aligned} -fv + g'\eta_x &= 0 \\ v_t + fu + g'\eta_y &= 0 \\ u_x + v_y &= 0 \end{aligned} \tag{3.45}$$

The meridional flow is in geostrophic balance and the horizontal motion is nondivergent. A single equation for the meridional velocity component readily follows:

$$v_{xt} + \beta v = 0 \tag{3.46}$$

This equation has solutions of the form $(\beta t/x)^{\nu/2} J_{\nu}(4x\beta t)$, where ν is a constant and J_{ν} is a Bessel function of order ν .

3.4.3 Kelvin Waves

Equatorial Kelvin waves have no meridional velocity fluctuations so that the equations of motion (3.1) simplify to

$$u_{tt} - c^2 u_{xx} = 0 \tag{3.47a}$$

$$fu_t - c^2 u_{xy} = 0 \tag{3.47b}$$

The first equation implies that

$$u = E(y)F(x \pm ct)$$

where E and F are arbitrary functions. Disturbances propagate nondispersively either eastward or westward with speed c . Equation (3.47b) determines the function E . It is unbounded at large values of y in the case of westward-propagating disturbances, which must therefore be ruled out. However, eastward equatorially trapped Kelvin waves are possible:

$$u = g'\eta/c = e^{-y^2/2\lambda^2} F(x - ct), \quad v = 0 \tag{3.48}$$

For the case of wave disturbances $F = \exp(ikx - i\sigma t)$, Eq. (3.47a) gives the dispersion relation

$$\sigma = ck \tag{3.49}$$

A disturbance that is symmetrical about the equator will disperse into an eastward-traveling Kelvin wave and a westward-traveling Rossby pulse as shown in Fig. 3.10.

A Kelvin wave packet is nondispersive so that its components are always in phase with each other and can interact nonlinearly⁴ in an efficient manner. Nonlinearities modify the equation

$$u_t + cu_x = 0 \quad (3.50)$$

in essentially two ways. Advection increases the phase speed from c to $c + u$. There is an additional change in the phase speed because of the deepening of the thermocline by the wave itself:

$$H \rightarrow H + \eta = H + cu/g' \quad (3.51)$$

$$\therefore c \rightarrow (g'H + cu)^{1/2} \sim c + u/2 \quad \text{for small } u/c$$

According to this heuristic argument (Ripa, 1982) these two nonlinear corrections amount to the replacement of c by $c + 3u/2$ in Eq. (3.53). The zonal current u is a function of latitude so that its effect has to be averaged in that direction. This procedure gives the following equation for the nonlinear Kelvin wave:

$$u_t + \left(c + \sqrt{\frac{3}{2}}u\right)u_x = 0 \quad (3.52)$$

Equation (3.54), which can be derived formally by means of a perturbation expansion provided $u/c \ll 1$, has a solution that can be written in parametric form (Ripa, 1982; Boyd, 1980a). Figure 3.11 shows this solution for a disturbance that initially is Gaussian:

$$u(x, t = 0) = A \exp(-x^2/2a^2) \quad (3.53)$$

The leading edge of the disturbance, which introduces eastward currents and deepens the thermocline as it propagates eastward, steepens until it forms a front after a time

$$t = \frac{a}{A} \left(\frac{2e}{3}\right)^{1/2}$$

This singularity can be avoided by permitting not only Kelvin waves but also Rossby or inertia-gravity waves in the interactions. A Kelvin pulse with an amplitude of +50 cm/sec and a zonal scale of 5000 km will steepen into a front after approximately 100 days—before it has crossed the Pacific if it were excited in the west. By that time its speed would have increased by almost 30%. If the amplitude were $A = -50$ cm/sec, so that the initial pulse elevates the thermocline, then nonlinearities decrease both the speed and zonal gradients across the pulse. Nonlinear effects such as these have been identified in numerical models and may contribute to discrepancies between observed and predicted Kelvin wave speeds.

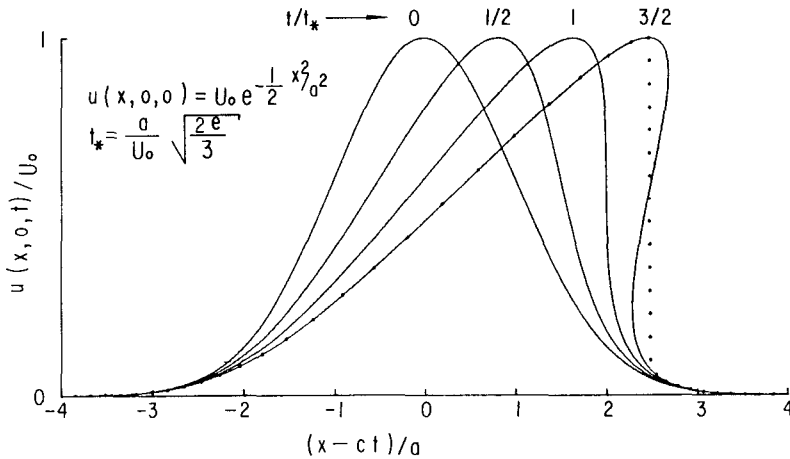


Figure 3.11. The nonlinear evolution of a pulse of Kelvin waves, associated with eastward currents and a depression of the thermocline. Initially, at time $t = 0$, the pulse is a Gaussian. The curves show the zonal structure of the eastward current at different times. The x axis is shifted for each curve in such a way that the departure from the initial curve is a nonlinear effect. The dots show the front at time $t = t^*$. [From Ripa (1982).]

Although observations that show eastward phase propagation along the equator are plentiful, it is difficult to find measurements that unambiguously show the presence of Kelvin waves. This is because the waves are superimposed on other waves and on time-dependent wind-driven currents (which have no dispersion relation). Measurements that filter out some of this variability provide the most persuasive evidence of Kelvin waves. Knox and Halpern (1982), for example, integrate the zonal currents vertically to reveal a pulse that propagated nondispersively from the central to the eastern equatorial Pacific in the northern spring of 1980 (Fig. 3.21). The vertical structure of the pulse changed significantly during its journey, presumably because of the presence of fluctuations not attributable to Kelvin waves. Tide gauges and Inverted Echo Sounders (which detect changes in the travel time of sound pulses through the water column) measure a vertical average of the density. This filter tends to bring Kelvin waves into prominence (Eriksen *et al.*, 1983; Katz, 1987a). As the 1982–1983 El Niño developed, tide-gauge records showed an eastward-traveling signal that appears to have been a first baroclinic mode Kelvin wave (Lukas *et al.*, 1984). Of far greater importance to the development of El Niño, however, was the considerably slower, eastward migration of isotherms on the ocean surface shown in Fig. 1.20. This migration, and more generally the development of all El Niño episodes, depends on far more than oceanic Kelvin

waves and involves the unstable ocean–atmosphere interactions described in Chapter 6.

Kelvin waves are possible along the equator and also along coasts. If the coast is north–south then the mathematical description of these waves is complex because of the latitudinal variation of the Coriolis parameter (Moore, 1968). Section 3.4.5 on reflections pursues this matter. The next topic concerns the effect of east–west coasts.

3.4.4 Coasts Parallel to the Equator

Consider a zonal coast at such a high latitude that the value of the Coriolis parameter is essentially a constant f_0 within a radius of deformation c/f_0 of the coast. Explore motion with no meridional velocity component so that Eqs. (3.47) are the governing equations with $f = f_0$. It follows that disturbances propagate nondispersively either eastward or westward along the coast with speed c . In the case of eastward-traveling waves, the amplitude grows exponentially with increasing distance from the coast at $y = L$. In the case of westward-propagating signals,

$$u = \exp[(y - L)f_0/c]f(x - ct) \quad (3.54)$$

The e -folding distance for these coastal waves is the local value of the radius of deformation. Their dispersion relation is

$$\sigma = -ck \quad (3.55)$$

These are coastal Kelvin waves that travel with the coast on their right in the Northern Hemisphere and on their left in the Southern Hemisphere.

If a zonal coast is near the equator then the properties of Kelvin waves along that coast are affected by the latitudinal variations of the Coriolis force. Such a coast will also affect the equatorially trapped waves. This can happen in the eastern tropical Atlantic, in the Gulf of Guinea, which has a coast near 5°N . Equation (3.19), which describes equatorial waves, must now be solved subject to the condition that $v = 0$ at 5°N . This means that the equatorial Kelvin wave is unaffected because it has no meridional velocity component. The dispersion relation for the other waves continues to be Eq. (3.32) but the integers n are replaced by positive eigenvalues μ_n ($n = 0, 1, 2, \dots$). The eigenfunctions are Parabolic Cylinder Functions. (When the coasts are far from the equator, at $\pm\infty$ then $\mu_n = n$ and the Cylinder Functions are Hermite functions.) The first few eigenvalues that correspond to the conditions $v = 0$ at 5°N and v bounded at $y = -\infty$ are (Cane and Sarachik, 1981)

$$\mu_0 = 0.01, \quad \mu_1 = 1.1, \quad \mu_2 = 2.2, \quad \mu_3 = 3.4, \quad \mu_4 = 4.8$$

The difference between μ_n and n is a measure of the degree to which the

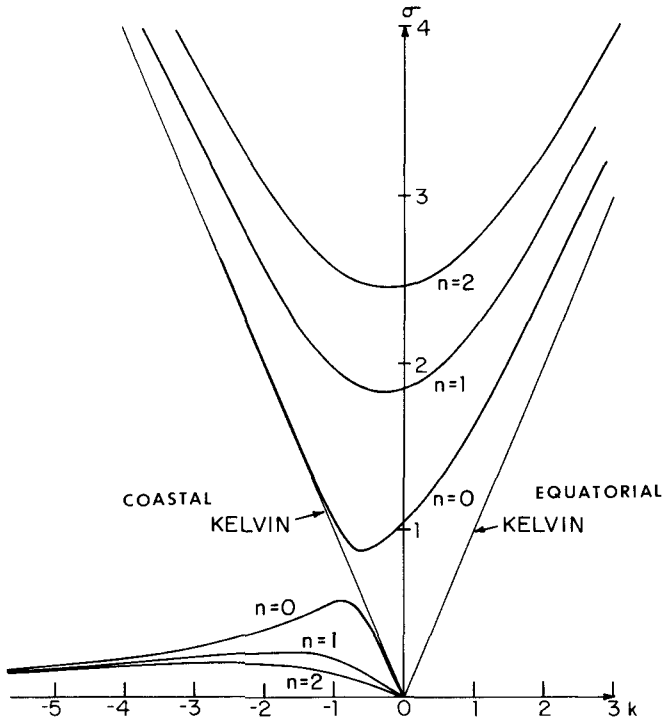


Figure 3.12. The dispersion diagram when a wall is present along a circle of latitude 1.7 radii of deformation north of the equator. This is the approximate location of the northern coast of the Gulf of Guinea. The unit of frequency is $(\beta c)^{1/2}$ and the unit of wave number k is $(\beta/c)^{1/2}$. The $n = 0$ Rossby-gravity curve of Fig. 3.8, which would have intersected the line for coastal Kelvin waves, now becomes two curves, for inertia-gravity-Kelvin and Rossby-Kelvin modes. [From Cane and Sarachik (1979).]

east–west coast affects the equatorial waves. The gravest mode appears to be little affected but the dispersion diagram (Fig. 3.12) indicates otherwise. Instead of a Rossby-gravity and coastal Kelvin wave there are Rossby-Kelvin and inertia-Kelvin modes. The structure of these modes, in the wave number range where they have westward group velocities and are nondispersive, resembles that of coastal Kelvin waves except that the meridional velocity component is not zero. Figure 3.13 shows the structure for a modified coastal Kelvin wave with frequency $\sigma = 0.5$ and zonal wave number -0.6 . [The unit of time is $(\beta c)^{-1/2}$ and the unit of distance is the radius of deformation.] The existence of this very rapid westward-propagating mode in the Gulf of Guinea could enable the northern part of the gulf to adjust very rapidly to changes in the winds.

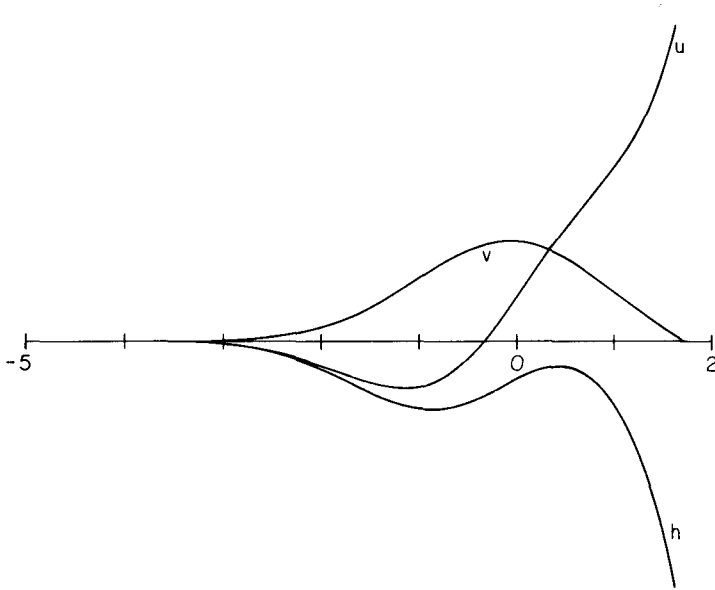


Figure 3.13. The structure of a Rossby-Kelvin mode for the point $\sigma = 0.5$, $k = -0.501$ in Fig. 3.12. The zonal velocity component (u) and thermocline depth (h) have maxima at the coast, as for coastal Kelvin waves, but the meridional velocity component (v) is nonzero. [From Cane and Sarachik (1979).]

3.4.5 Reflections at Eastern Coasts

The dispersion diagram (3.8) is strikingly asymmetrical about the $k = 0$ axis at subinertial frequencies. At periods from a week to a month only Kelvin and Rossby-gravity waves are possible and their group velocities are strictly eastward. Therefore energy accumulates at the eastern sides of equatorial ocean basins at these periods because waves with westward group velocities are unavailable for the westward reflection of energy. The wave numbers k of the waves that ought to be available for reflection can be calculated from the dispersion relation (3.32):

$$k = -\frac{\beta}{2\sigma} \pm \frac{1}{2} \left[\frac{\beta^2}{\sigma^2} - 4 \left(\beta \frac{2n+1}{c} - \frac{\sigma^2}{c^2} \right) \right]^{1/2} \quad (3.56)$$

At frequencies close to $(\beta c)^{1/2}$ —periods between a week and a month—the wave numbers k have complex values for all values of n . Since oscillations are assumed to have x dependence of the form $\exp(ikx)$, this result implies that a disturbance incident on an eastern boundary at $x = L$ excites coastally trapped waves. Far from the equator, for y large and positive, the

sum of the coastally trapped disturbances asymptote to the expression

$$v = Ay^{1/2} \exp \left[i \left(\sigma t - \frac{\sigma y}{c} + \frac{\beta x}{2\sigma} \right) - \beta y \frac{L-x}{c} \right] \quad (3.57)$$

where A is a constant. This expression resembles a coastal Kelvin wave: it propagates poleward at speed c and is confined to a coastal zone with a width equal to that of the local radius of deformation $c/\beta y$. Although this width decreases with increasing latitude, the amplitude of the wave ($\sim y^{1/2}$) increases with increasing latitude so that energy is conserved. The wave differs from the coastal Kelvin wave of Eq. (3.50) because the velocity component normal to the coast is not zero and because the lines of constant phase are not normal to the coast. Similar waves are possible along the western sides of ocean basins where they propagate equatorward (Moore, 1968).

Analyses of sea level measurements along the western coasts of North and South America confirm the presence of coherent poleward-propagating disturbances, some of which are correlated with wind fluctuations over the equatorial Pacific Ocean (Enfield and Allen, 1980).

At frequencies near $(\beta c)^{1/2}$, Kelvin or Rossby-gravity waves incident on an eastern boundary excite only coastally trapped waves as shown in Fig. 3.8. As the frequency of the incident wave decreases, an increasing but always finite number of long Rossby waves become available for reflection. In Eq. (3.56) these waves are associated with the low values of n for which k is real. For large values of n , k is complex so that reflection involves a finite number of Rossby waves and an infinite number of coastally trapped waves. This means that there is always a poleward loss of energy at the eastern coast. This loss decreases with decreasing frequency. At very low frequencies the loss is negligible and an incident Kelvin wave of the form

$$u = \exp \left(-\frac{y^2}{2\lambda^2} \right) \cos \sigma \left(t - \frac{L-x}{c} \right)$$

reflects as long nondispersive Rossby waves (Eq. (3.44)). The sum of the incident and reflected waves can be written as (Cane and Moore, 1981)

$$\begin{aligned} u &= -i\eta \tan(s) \\ v &= i\sigma\eta y \sec 2(s) \\ \eta &= \cos^{1/2}(s) \exp \left[i\sigma t + \frac{y^2}{2\lambda^2} \tan(s) \right] \end{aligned} \quad (3.58)$$

where

$$s = 2\sigma(x-L)/c$$

These expressions are singular at $s = \pi/2, 3\pi/2, \dots$, which are foci similar to those of Eq. (3.31) and Fig. 3.7.

The results of Eq. (3.58) can be used to determine the reflection of a Kelvin wave front or bore at an eastern coast. Let the incident front be described by

$$u = S(x - ct)\exp(-y^2/2\lambda^2)$$

where $S(x - ct)$ is a step function so that $S = 0$ if $x < ct$ and $S = 1$ if $x > ct$. As the front propagates eastward into a motionless region it suppresses the thermocline and introduces a steady, geostrophic eastward jet. At the eastern boundary the front excites poleward-traveling coastal waves that initially are trapped within a radius of deformation of the coast. With time, westward Rossby dispersion becomes possible (Anderson and Rowlands, 1976b). According to Eq. (3.57) this happens after a time $(2y/c)^{1/2}$ at a latitude y . The dispersion steadily increases the width of the coastal zone, more rapidly in low than in high latitudes because Rossby waves travel faster near the equator. After a long time the effect of all the reflected Rossby waves is to cancel the zonal current associated with the incident equatorial Kelvin front and to lower the thermocline uniformly everywhere (Cane and Sarachik, 1977). This asymptotic state is described by Eq. (3.58) in the limit $\sigma \rightarrow 0$:

$$u = v = 0; \quad \eta = \sqrt{2} \quad (3.59)$$

3.4.6 Reflections at Western Coasts

The reflection of waves incident on the western boundary of an ocean basin involves a Kelvin or Rossby-gravity wave, depending on the symmetry of the incident wave. Because of this, reflection at a western boundary, unlike that at an eastern, is not associated with a poleward loss of energy. Consider a Rossby wave with meridional wave number N and frequency σ that is incident on a western coast at $x = 0$. In Eq. (3.56) the wave number of the incident wave corresponds to the plus sign for which group velocities are westward. The minus sign is appropriate for the reflected waves that have eastward group velocities. A recursive relation for the amplitude of the reflected waves can readily be written down (Moore and Philander, 1977); the solution has a number of important properties. The reflected waves are finite in number and have meridional wave numbers n that are all less than that of the incident wave. In other words, the incident wave reflects as a finite number of short Rossby waves plus a Kelvin or Rossby-gravity wave. The zonal wave numbers k of the reflected waves are all real so that the reflection does not involve coastally trapped waves. (Coastally trapped

waves come into play when coastal Kelvin waves along the northern or southern coast are incident on the western coast or when they are excited by forcing along the western coast.) The Hermite functions D_n that describe the reflected waves all have $n < N + 1$, where N is the meridional wave number of the incident wave. This means that the reflected wave is at least as equatorially trapped as the incident wave.

At very low frequencies, reflections at western boundaries involve the short Rossby waves described by Eqs. (3.45). These nondivergent waves redistributed mass meridionally but they are not associated with a net zonal mass flux. Zonal mass flux into the western boundary is therefore returned eastward by the only other wave with an eastward group velocity, the equatorial Kelvin wave. This wave returns all the mass incident on the western coast, but it does not return all the energy incident on that coast. Suppose that the mass and energy flux incident on the western coast are associated with a long Rossby wave of meridional mode number N . At frequencies sufficiently low for Eqs. (3.45) to be valid, the fraction R of the energy flux [see Eq. (3.38)] returned eastward by the Kelvin wave is (Clarke, 1983)

$$R = 0.5, \quad N = 1$$

$$R = \frac{(N - 2)(N - 4) \dots 1}{(N + 1)(N - 1)(N - 3) \dots 2}, \quad N = 3, 5, 7, \dots \quad (3.60)$$

At most half the energy of the gravest equatorially trapped Rossby mode returns eastward as a Kelvin wave. In the case of an incident wave that is antisymmetrical about the equator, there is no meridionally integrated mass flux into the western coast $x = 0$, no Kelvin wave is excited, and short Rossby waves transport mass across the equator in a western boundary current. (The energy flux ratio R is zero in this case.)

Reflections of Rossby waves off the western boundary of the Pacific Ocean are critically important in some coupled ocean-atmosphere models of the Southern Oscillation (Chapter 6). The Pacific of course does not have a continuous western boundary but if it is assumed that New Guinea, Irian Jaya, and Maluka form a barrier to westward-traveling equatorial Rossby modes then the slope of this barrier to meridians will affect reflections. In the Indian and Atlantic Oceans the coasts also slope relative to meridians. The condition that the incoming mass flux normal to the coast due to long Rossby waves must be returned by a Kelvin wave determines the reflections (Cane and Gent, 1984). Equatorial Kelvin waves can now be excited by Rossby waves that are symmetrical about the equator and also by those that are antisymmetrical. For the western equatorial Pacific it is estimated that the amplitude of reflected Kelvin waves is reduced on the order of 30%

from that which would be achieved if the boundary coincided with a meridian.

The higher the meridional mode number of equatorially trapped Rossby waves, the larger the number of zeroes of the zonal velocity component and the smaller the meridionally integrated zonal mass flux. This is why the amplitude of the reflected Kelvin wave is small. A disturbance with a large zonal mass transport that is incident on a western coast at a relatively high latitude, near 15°N say, will give rise to an equatorial Kelvin wave with the same mass flux even though each of the Rossby waves, whose sum describes the disturbance, will excite a Kelvin wave with a relatively small amplitude. It is the mass transport normal to the coast that matters.

3.4.7 Basin Modes

Figure 3.14 depicts the structure of one class of resonant modes of a closed ocean basin. The period is approximately the time it takes equatorial and coastal Kelvin waves to travel around the basin, clockwise in the Southern Hemisphere and anticlockwise in the Northern Hemisphere. (Allowance must be made for the time it takes Kelvin waves to turn corners.) The period of this class of modes must be close to $P = 2\pi(\beta c)^{-1/2}$ for the mode to involve only equatorial and coastal Kelvin waves. As the difference between P and the resonant period increases, Rossby (or inertia-gravity) waves come into play and the width of the equatorial zone in Fig. 3.14

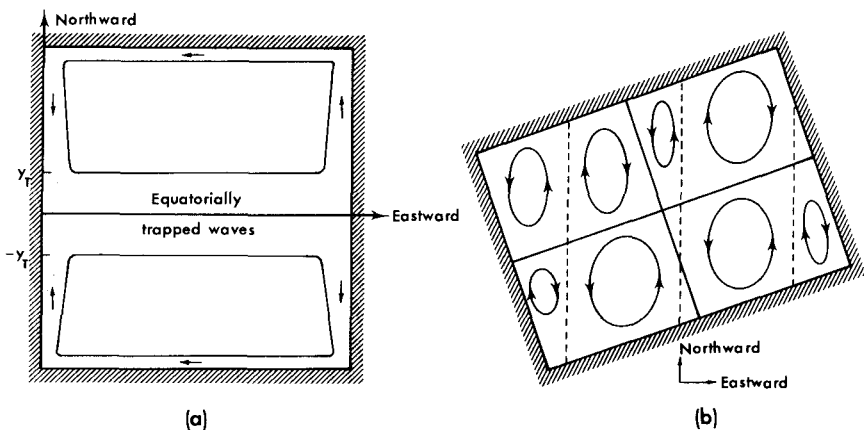


Figure 3.14. The structure of the modes of an ocean basin at frequencies (a) close to $\sigma_0 = (2\beta c)^{1/2}$ and (b) much lower than σ_0 . In case (a) there is eastward phase propagation along the equator as Kelvin waves are the only equatorially trapped waves that are excited. In case (b) there are fixed nodal lines (the straight solid lines) and westward-propagating phase lines (the dashed lines).

widens. At very low (or high) frequencies it is possible to have modes without distinctive equatorial or coastal zones. Figure 3.14b shows the structure of such a low-frequency mode, which is a superposition of Rossby waves with eastward and westward group velocities (Moore, 1968). Low-frequency resonant modes of an ocean basin generally involve short Rossby waves with eastward group velocities. As noted earlier, the slow speeds and short scales of these waves make them prone to dissipation. A mode composed solely of equatorial Kelvin and long Rossby waves is therefore of special interest. Equation (3.58), which describes the sum of a Kelvin wave incident on an eastern coast ($x = L$) plus the long Rossby waves reflected there, also satisfies the condition $u = 0$ at a western ($x = 0$) wall provided (Cane and Moore, 1981)

$$P = 2\pi/\sigma = 4L/cm, \quad m = 1, 2, 3, \dots \quad (3.61)$$

For $m = 1$ this period is the time L/c it takes an equatorial Kelvin wave to propagate eastward across the basin, plus the time $3L/c$ it takes the gravest equatorially trapped Rossby wave to travel westward across the basin. In a shallow-water model this mode is excited by an abrupt intensification of the wind (Section 3.6).

3.4.8 Islands

The Gilbert and Galápagos Islands in the Pacific Ocean, and the Maldives in the Indian Ocean, fail to reflect or impede equatorial waves primarily because these islands have a latitudinal scale that is small relative to the equatorial radius of deformation (Yoon, 1981; Cane and du Penhoat, 1981; Rowlands, 1982). Small islands can and have been used as instrument platforms that do not affect the waves. Sea level measurements on the western side of the Galápagos Islands confirm the latitudinal structure of equatorial Kelvin waves (Ripa and Hayes, 1981). Even an island with a large latitudinal extent will fail to impede Kelvin waves with a frequency close to $(\beta c)^{1/2}$ because the coastally trapped waves excited at the island will propagate as shown in Fig. 3.15 and will regenerate eastward-traveling equatorial Kelvin waves.

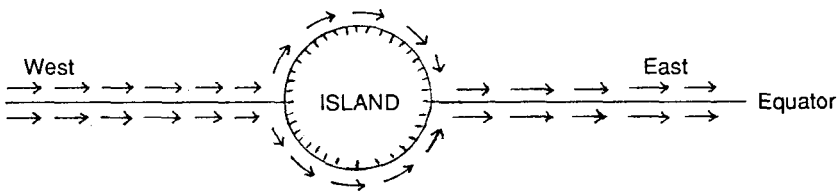


Figure 3.15. A schematic of Kelvin waves propagating around an island.

3.5 Generation of Sverdrup Flow

The mean surface currents in the tropical Pacific Ocean, except for those within a radius of deformation of the equator, are to a reasonable approximation in accord with the Sverdrup balance (3.9). These currents, shown in Fig. 2.1, have considerable seasonal and interannual variability. Assume that this variability is described by Eq. (3.8). A scale analysis of this equation yields interesting information about the oceanic response to variable winds in different frequency ranges. The ratio of the two terms on the left-hand side of the equation defines a time scale T where

$$T^2 = f^2 L / \beta c^2 = 2aL\Omega \sin^2 \theta / c^2 \cos \theta \quad (3.62)$$

Latitude is denoted by θ . If the time scale of the wind fluctuations is T^* then the oceanic response depends critically on the ratio T to T^* .

$T^* \ll T$ and $T \gg 1/f$: At high frequencies, wind fluctuations do not excite Rossby waves because the term $(\beta\psi_x)$ in Eq. (3.8) is negligible. The response is local and the divergence of the Ekman drift determines vertical movements of the thermocline.

$T^* \sim T$: On time scales comparable to T the response is nonlocal because Rossby waves are important.

$T^* \gg T$: At low frequencies the first term in Eq. (3.8) is negligible and the oceanic response is a Sverdrup flow that is in phase with the slowly varying winds. The ocean is always in equilibrium with the winds and in effect passes through a succession of steady states.

If the forcing is at a fixed frequency, at a period of one year, say, so that $T^* = 1$ year, then the inequalities stated above define bands of latitude in which the oceanic response changes. In low latitudes, where T has a small value, $T^* \gg T$ and the response is equilibrium Sverdrup flow; at higher latitudes, where T has a longer value, Rossby wave propagation is evident; and farther north, local Ekman suction determines the vertical movements of the thermocline.

The time T , which is the time L/s it takes long Rossby waves with speed s to propagate a distance L , is the adjustment time of the ocean. To demonstrate this explicitly consider how the ocean adjusts to winds that suddenly start to blow and then remain steady. To simplify matters assume that the forcing has the latitudinal structure $\sin(ny)$ so that Eq. (3.8) after an appropriate redefinition of ψ becomes

$$(\psi_{xx} - r^2\psi)_t + \beta\psi_x = A \quad (3.63)$$

where

$$r^2 = n^2 + f_0^2/c^2$$

If the winds, which have a constant curl A , are assumed to be zonal then they can be viewed as an idealization of the winds that drive the subtropical gyre: westerly winds north of 30°N , say (where $y = 0$ and $f = f_0$), and easterly winds to the south of this latitude. These winds start to blow suddenly at time $t = 0$ and then remain steady. The oceanic response can be written

$$\psi = \psi^I + \psi^{\text{LR}} + \psi^{\text{SR}}$$

where ψ^I is the initial response in the oceanic interior, far from coasts. This response is independent of longitude:

$$\psi^I = -At/r^2 \quad (3.64)$$

This steady vertical movement of the thermocline is caused by the divergence of the Ekman drift. Associated with this displacement of the thermocline is an accelerating geostrophic zonal current u ($= (g'/f_0)n\psi \cos ny$) that satisfies the boundary conditions on neither the western ($x = 0$) nor eastern ($x = L$) coasts. To meet the boundary conditions it is necessary to superimpose on the particular integral (3.64) the free modes, namely Rossby waves. [All other waves are filtered from Eq. (3.8).] At the eastern coast, Rossby waves ψ^{LR} with westward group velocities are excited. Assume that these waves are long so that they satisfy the hyperbolic equation

$$-r^2\psi_t^{\text{LR}} + \beta\psi_x^{\text{LR}} = 0$$

so that

$$\psi^{\text{LR}} = F(x + \beta t/r^2)$$

where F is a function which satisfies the equation

$$\begin{aligned} F(L + \beta t/r^2) &= 0 & \text{for } t < 0 \\ &= At/r & \text{for } t > 0 \end{aligned} \quad (3.65)$$

It follows that

$$\begin{aligned} \psi^I + \psi^{\text{LR}} &= -At/r^2 & \text{for } t < r^2(L - x)/\beta \\ &= -A(L - x)/\beta & \text{for } t > r^2(L - x)/\beta \end{aligned} \quad (3.66)$$

This equation describes a dramatic change in the motion, from an accelerating zonal current to steady Sverdrup flow:

$$v = \psi_x = A/\beta = \text{curl}_z \tau \quad (3.67)$$

This happens after a time $t = (L - x)r^2/\beta$, which is how long it takes a long nondispersive Rossby wave to travel from the wall at $x = L$ to the point x . West of the front the accelerating flow is strictly zonal but to the

east of the front the Sverdrup flow has a meridional component given by Eq. (3.67). Since the flux across a circle of latitude must be zero in an ocean basin, the southward flux east of the front returns northward in the discontinuity at the front.

To satisfy the boundary conditions at the western coast $x = 0$ it is necessary to invoke short Rossby waves ψ^{SR} with eastward group velocities. Under the assumptions already made these waves satisfy Eqs. (3.45). The solution that satisfies the boundary condition at $x = 0$ and that merges with the interior solution (3.64) is

$$\psi^{\text{I}} + \psi^{\text{RS}} = Ar^{-2} \left[-t + \left(\frac{t}{\beta x} \right)^{1/2} J_1(2\sqrt{\beta xt}) \right] \quad (3.68)$$

At this stage three regimes characterize the oceanic response: a western boundary current described by Eq. (3.68); an interior region where the zonal current accelerates according to Eq. (3.64); and an eastern region where the westward-expanding Sverdrup balance given by Eq. (3.66) obtains. In due course—in the time it takes a long Rossby wave to propagate westward across the basin—the solution in Eq. (3.68) is inappropriate because the western boundary layer must merge, not with the accelerating zonal current, but with the Sverdrup balance, which is now established across the entire basin. Motion is now described by the expression

$$\begin{aligned} \psi &= \psi^{\text{I}} + \psi^{\text{RS}} + \psi^{\text{LR}} \\ &= -\frac{AL}{\beta} \left[1 - x/L - J_0(2\sqrt{\beta xt}) \right] \end{aligned} \quad (3.69)$$

Far from the western coast there is steady Sverdrup flow. If the width of the western boundary current is taken to be the first zero of the Bessel function J then this width decreases with increasing time. However, the thinning current must return northward the Sverdrup transport $\int_0^L A dx$ that flows southward across a circle of latitude. It follows that the speed of the western boundary current must increase as its width decreases—this is evident in the solution shown in Fig. 3.16—so that the vorticity v_x in the western boundary increases steadily. The wind imparts vorticity uniformly over the basin but it accumulates near the western coast, where a singularity develops with increasing time. Friction can be invoked to dissipate the vorticity near the coast (Stommel, 1948), but measurements do not show high levels of dissipation underneath the Gulf Stream, for example. A realistic alternative is to permit the western boundary current to become unstable, because of its shear. In that case the equilibrium response to steady winds is steady Sverdrup flow except for an unstable time-dependent

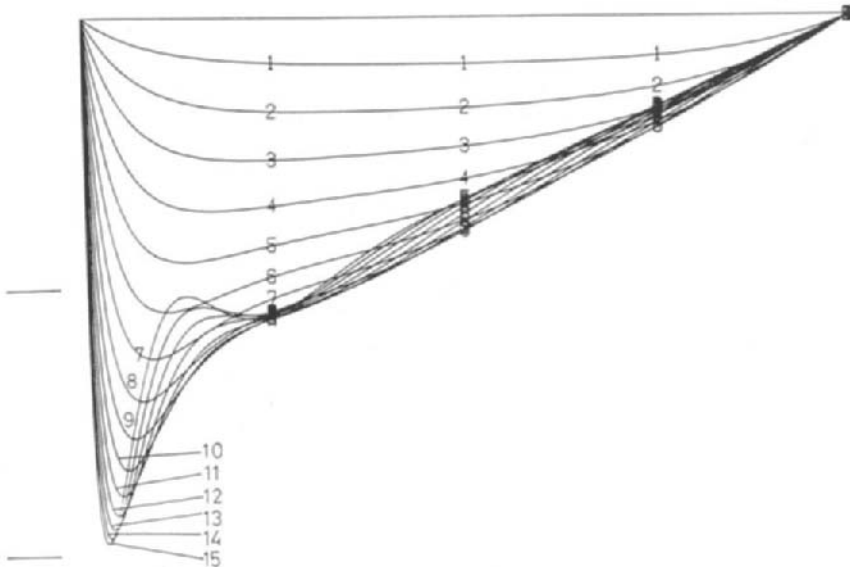


Figure 3.16. Displacements of the thermocline at different times (marked 1 to 15) after the wind turns on at time zero over an ocean initially at rest. In the center of the basin, Ekman pumping at first deepens the thermocline until the arrival of long Rossby waves from the east arrests the deepening and establishes a Sverdrup balance so that the thermocline has a zonal slope. The western boundary current becomes thinner and more intense with increasing time. [From Anderson and Gill (1975).]

western boundary current. Waves radiated by this current can be dissipated in regions remote from the current.

The time it takes the ocean to return to a state of equilibrium after a sudden change in the winds is essentially the time it takes a long Rossby wave to propagate from east to west across the basin of width L and is given by Eq. (3.62). This adjustment time decreases rapidly with decreasing latitude, as shown in Fig. 3.5, so that it takes far longer to generate, from rest, midlatitude currents such as the Gulf Stream than low-latitude currents such as the Somali Current or those in Fig. 2.1. Measurements indicate that the time it takes the ocean to adjust to a change in the winds is indeed shorter in low than in high latitudes. There have also been attempts to compare measurements with the solutions of Eqs. (3.8) and (3.63) in a more quantitative manner. In studies of the North Equatorial Countercurrent in the Pacific (Meyers, 1980) and Atlantic (Garzoli and Katz, 1983; Katz, 1987b), seasonal vertical movements of the thermocline have been explained in terms of Rossby waves near the southern boundary of the current and local Ekman suction near 10°N , consistent with the analysis of

Eq. (3.63). This agreement between measurements in low latitudes and the solution to Eq. (3.63) is a puzzle because some of the conditions that have to be satisfied for (3.63) to be valid are violated. For example, the assumption that the waves that effect the oceanic adjustment have a constant north–south wave number requires that the value of the Coriolis parameter f be relatively constant. This is a poor assumption in a latitude as low as 10°N . If variations in f are taken into account then the waves propagate not with a fixed but with a variable north–south wave number. This results in Rossby wave dispersion such as that shown in Fig. 3.7. It follows that the waves excited near one meridian will fail to reach certain parts of the ocean because of refraction. In these shadow zones a Sverdrup balance is impossible and local Ekman pumping determines thermocline movements. Along 10°N there ought to be shadow zones between certain meridians while Rossby waves should be evident in other regions. If this is not observed then other factors, such as the presence of mean currents, must come into play. The point is that Eq. (3.63) is not valid in the region of the North Equatorial Countercurrent. The apparent agreement that has thus far been found between the measurements and the theory is perplexing, not reassuring. The matter is pursued in Section 3.9.

The expression for the adjustment time of the ocean in Eq. (3.62) is singular at the equator because the approximations that were made in the derivation of this equation become invalid. Neglected factors that are important close to the equator include the change in the dispersion relation for Rossby waves, the existence of Kelvin waves, and the equatorial jet that can be generated by winds parallel to the equator.

3.6 Equatorial Adjustment

Near the equator the sudden onset of spatially uniform zonal winds at first generates the accelerating equatorial jet described in Section 3.3. Ultimately the zonal winds maintain a pressure gradient while the ocean approaches a state of rest (Eq. (3.10)). The adjustment from the initial state to the final equilibrium state is effected by the waves discussed in Section 3.4. In the case of a nonrotating tank of water, only gravity waves are available for the adjustment, but in the case of a rotating spherical shell of fluid, the gravity waves can be completely unimportant. This is because the inertia-gravity waves have periods strictly less than a week [$2\pi(2\beta c)^{-1/2}$ near the equator]. It follows that if the onset of the winds is gradual so that they attain full strength after a week or two, then the winds excite practically no inertia-gravity waves. Assume that the winds behave in this manner. Kelvin and Rossby waves are then responsible for the oceanic adjustment so that

the motion at any moment is a superposition of these waves and the wind-driven jet described by Eq. (3.16):

$$u = u^{\text{JET}} + u^{\text{K}} + u^{\text{R}} \quad (3.70)$$

The superscripts K and R indicate Kelvin and Rossby waves. The amplitudes of the waves are determined by the boundary conditions at the meridional coasts:

$$u = 0 \quad \text{at } x = 0 \text{ and } L \quad (3.71)$$

Only waves with eastward group velocities are excited at the western boundary $x = 0$. The short, slow Rossby waves, as pointed out in Section 3.4, are important only near this coast where they redistribute mass meridionally (alongshore). They do not transport mass zonally at low frequencies so that the Kelvin wave is solely responsible for returning eastward any westward mass flux into the coast (Cane and Sarachik, 1977):

$$\int_{-\infty}^{\infty} u^{\text{JET}} dy = - \int_{-\infty}^{\infty} u^{\text{K}} dy \quad \text{at } x = 0 \quad (3.72)$$

This condition determines the function F in the expression for the Kelvin wave in Eq. (3.48):

$$\begin{aligned} F(-ct) &= 0 & \text{for } t < 0 \\ &= -\alpha t \tau^x / H & \text{for } t > 0 \end{aligned}$$

It follows that

$$\begin{aligned} u^{\text{K}}(x, y, t) &= 0 & \text{for } t < x/c \\ u(x, y, t) &= \frac{\alpha \tau^x}{cH} (x - ct) \exp(-y^2/2\lambda^2) & \text{for } t > x/c \end{aligned} \quad (3.73)$$

where α is a constant with a value of 0.84. This expression describes a front or bore that is excited at the western coast at time $t = 0$ and that propagates eastward at speed c . The front dramatically changes the initial response of the ocean to the zonal winds: in the wake of the front there is a sharp reduction in the acceleration of the zonal jet and in the intensity of the equatorial upwelling:

$$u = \tau^x x / Hc \quad \text{on } y = 0 \text{ for } t > x/c \quad (3.74)$$

This happens because the front introduces a steady zonal pressure gradient that balances the windstress:

$$\eta_x = \frac{\alpha \tau^x}{H} \exp(-y^2/2\lambda^2) \quad (3.75)$$

In the wake of the front the zonal momentum balance near the equator

changes from $u_t = \tau^x/H$ to $g'\eta_x \sim \tau^x/H$. The front also causes the jet to become horizontally divergent so that the poleward Ekman drift is no longer maintained by equatorial upwelling: the equation for the conservation of mass changes from $\eta_t + hv_y = 0$ to $H(u_x + v_y) \sim 0$.

Consider next the waves with westward group velocities that are excited at the eastern coast. Of most importance are the long nondispersive Rossby waves

$$u^R = \frac{\tau^x}{cH} \sum_n \alpha_n S[x - L + ct/(2n + 1)] R_n(y) \quad (3.76)$$

where R_n describes the latitudinal structure of the n th Rossby mode, which is given by Eq. (3.36) with $\sigma = -ck/(2n + 1)$. The function S has the property $S(x) = 0$ if $x < 0$ and $S(x) = x$ if $x > 0$. The constants α_n are chosen such that the sum in Eq. (3.76) is equal to the expression for the equatorial jet [Eq. (3.16)]. The westward-traveling Rossby wave fronts, like the eastward-traveling Kelvin wave front, modify the equatorial jet by introducing zonal gradients. The Rossby waves, however, can extend to high latitudes, whereas the Kelvin wave affects only a region within a radius of deformation of the equator. The most rapid Rossby wave travels at speed $c/3$ and influences a narrow equatorial zone. The other Rossby modes travel more slowly, at speeds $c/7$, $c/11, \dots$, but they extend to higher latitudes. Far from the equator the initial motion is predominantly meridional Ekman drift $v = \tau^x/fH$. The long Rossby waves that emanate from the eastern coast ultimately eliminate both components of the horizontal flow so that the zonal wind maintains the pressure gradient of Eq. (3.10). The farther from the equator, the longer it takes to attain this equilibrium state. Figure 3.17 shows schematically how the oceanic adjustment proceeds: the initial response, an accelerating equatorial jet, persists longest in region I; a Kelvin front introduces steady motion in region II; westward-traveling Rossby fronts affect region III similarly; and very short Rossby waves are important in the western boundary layer IV.

After a time $3L/4c$ the Kelvin and Rossby fronts meet at the meridian $x = 3L/4$. There is now a zonal pressure gradient all along the equator, and the equatorial jet is practically steady at all meridians. The jet now starts to decelerate in the wake of the Kelvin front that propagates into the region already affected by the Rossby front, and similarly in the wake of the Rossby front as it propagates into the region $x < 3L/c$. Figure 3.18 clearly shows how the motion changes after the passage of the fronts. The Kelvin front incident on the eastern boundary at time L/c excites a new set of westward-traveling Rossby fronts. Subsequently there are repeated reflections at both coasts as fronts propagate back and forth. Each reflection at

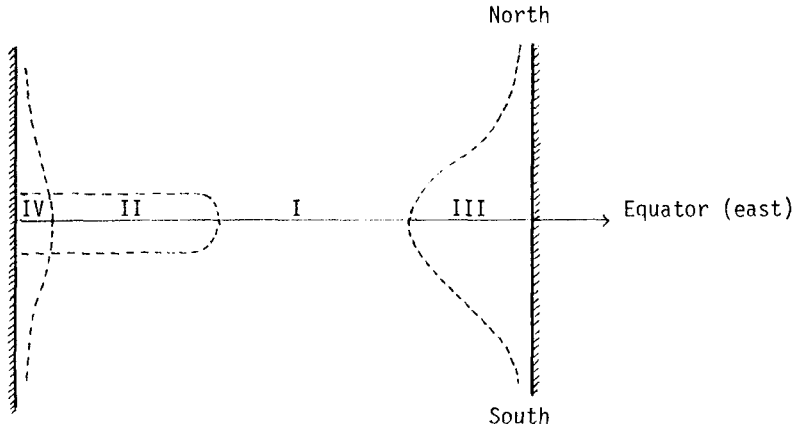


Figure 3.17. Schematic diagram that shows the distinct regions that characterize the oceanic adjustment to a sudden change in the winds.

the eastern boundary results in a loss of energy to high latitudes. Because of this the kinetic and potential energies of the equatorial region approach their equilibrium values rapidly.

Figure 3.19 shows that the adjustment time for the equatorial zone is, for practical purposes, $4L/c$, the time it takes a Kelvin wave to propagate eastward across the basin plus the time for the reflected Rossby wave to travel back westward across the basin. [This time $4L/c$ is also the period of the oscillations in the potential energy in Fig. 3.19 and is the period of the resonant equatorial mode of Eq. (3.61).]

The adjustment time of the ocean—the time it takes to establish equilibrium conditions after the sudden onset of steady winds—depends on the width of the basin and on latitude as shown in Fig. 3.5. Outside the equatorial zone the adjustment proceeds from the eastern coast and is effected by long Rossby waves as described in Section 3.5. Equation (3.62) gives the approximate adjustment time for that region. For the equatorial zone it is $4L/c$. For the Pacific Ocean the adjustment time is of the order of a decade in midlatitudes and decreases to approximately 450 days near the equator. The width of the equatorial Atlantic is only 5000 km, one-third that of the equatorial Pacific, so that its adjustment time is approximately 150 days. (The proximity of the northern coast of Brazil and the northern coast of the Gulf of Guinea to the equator probably reduces this estimate as mentioned earlier.)

Once the inviscid ocean is in equilibrium with steady, spatially uniform winds, it is motionless and has a sloping thermocline with which is associated a zonal pressure gradient that balances the wind. Suppose that the

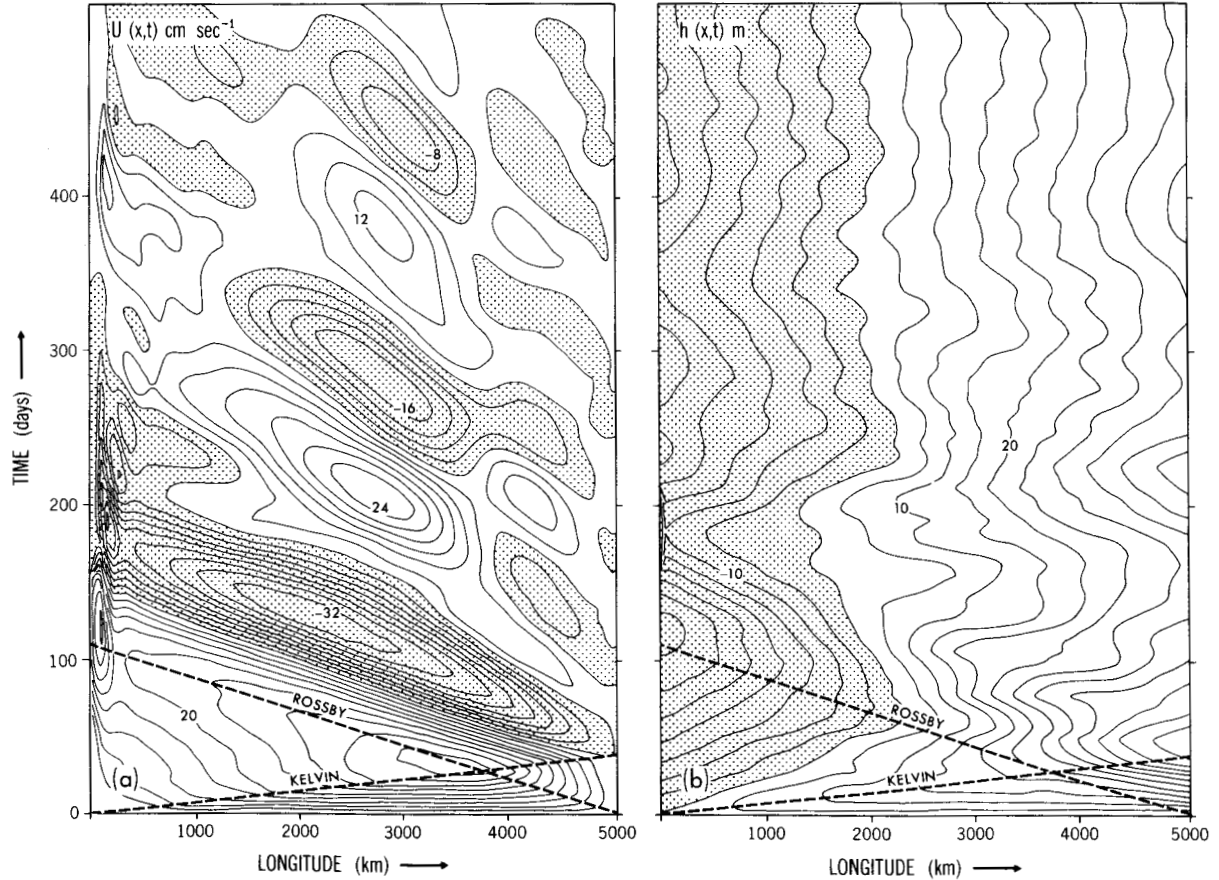


Figure 3.18. Changes in the zonal velocity component (centimeters per second) and in departures from the mean depth of the thermocline along the equator after the sudden onset of spatially uniform eastward winds. The dashed lines indicate the speeds at which Kelvin and the gravest Rossby mode propagate. The thermocline is elevated and motion is westward in shaded areas.

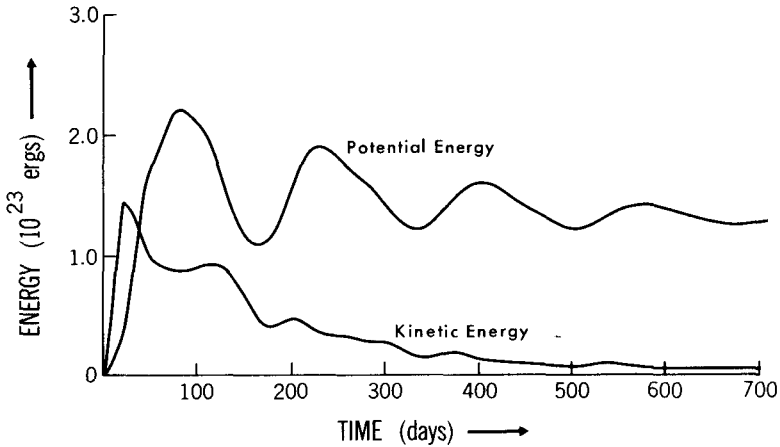


Figure 3.19. The kinetic and potential energy for the latitude band 5°N to 5°S for the motion in Fig. 3.18.

winds at this stage suddenly stop blowing. The pressure force will be left unbalanced and will initially accelerate the fluid in a direction opposite to that in which the wind had been blowing. The oceanic adjustment, back to a motionless state in which the thermocline is horizontal, will proceed exactly as before: waves excited at the coast will eliminate the zonal pressure gradient. This response to winds that suddenly stop blowing should be contrasted with the response (discussed in Section 3.3) of a zonally unbounded ocean to a similar change in the winds.⁵

3.7 Response to Remote Forcing

The winds over the ocean vary spatially, a factor not taken into account in the analysis thus far. To determine some of the effects associated with this complication, assume that the ocean is zonally unbounded and that spatially uniform eastward winds suddenly start to blow at time $t = 0$, but only between meridians A at $x = 0$ and B at $x = L$. There is no wind over the regions $x < 0$ and $x > L$.

The response is composed of a wind-driven equatorial jet between A and B —it is similar to the jet described in Section 3.3—plus Kelvin and Rossby waves excited at A and B to ensure continuity of the zonal velocity component and of the thermocline displacements at A and B . In the forced region, between A and B , the Kelvin front from A and the Rossby fronts from B introduce zonal pressure gradients that balance the windstress so

that the initial acceleration of the jet stops. The early evolution of the flow is therefore similar to that described in Section 3.6. In the absence of north–south walls from which waves reflect, there is no further adjustment so that the final equilibrium state includes a steady zonal jet (McCreary, 1976; Cane and Sarachik, 1977):

$$u = \frac{\tau^x L}{\sqrt{2} Hc} \exp(-y^2/2\lambda^2) \quad (3.77)$$

$$\eta = \frac{\tau^x}{c^2} \left(x - L + \frac{L}{\sqrt{2}} \exp(-y^2/2\lambda^2) \right), \quad 0 < x < L \quad (3.78)$$

The eastern unforced region ($x > L$) is motionless and has a horizontal thermocline until the arrival of the Kelvin front excited initially at B . This front introduces an accelerating equatorial jet and a steadily deepening thermocline that has a constant zonal slope:

$$u = -\frac{\tau^x}{Hc} (x - L - ct) \exp(-y^2/2\lambda^2)$$

$$\eta = -cu/g', \quad x > L; t > (x - L)/c \quad (3.79)$$

At a fixed point these conditions persist until the arrival of the second Kelvin front excited at A . This front arrests the acceleration of the jet, stops the deepening of the thermocline, and eliminates the slope of the thermocline. The winds between A and B therefore maintain a steady jet and a deepened thermocline to the east of B in a region that steadily expands eastward:

$$u = \frac{\tau^x L}{\sqrt{2} Hc} \exp(-y^2/2\lambda^2), \quad x > L; t > x/c \quad (3.80)$$

In the region to the west of B , where Rossby waves excited at A and B introduce an eastward jet and alter the topography of the thermocline, the latitudinal structure of the flow is more complex than in the east but the temporal evolution is similar.

The effect of a meridional boundary to the east of $x = L$ can be calculated by using the results of Section 3.4. From Eq. (3.58), which describes the long-term effect of a Kelvin front incident on an eastern boundary, it can be inferred that reflections at an eastern boundary will ultimately eliminate the equatorial jet established by the Kelvin waves in the region east of B but will leave the thermocline deeper than it originally was:

$$u = v = 0$$

$$\eta = \sqrt{2} \tau^x L / Hc, \quad x > L, t \gg x/c \quad (3.81)$$

Figure 3.20 shows changes in the depth of the thermocline in response to winds with a limited zonal extent. After a long time the thermocline is seen to have a slope in the forced region only. The uniform deepening of the thermocline to the east of the forced region gradually spreads poleward along the coast.

If the eastward winds, over a region with a zonal extent L , last for a time T , and if these winds start and stop abruptly, then the region to the east is affected by four Kelvin waves: two are excited at the extremes of the forced region when the winds start to blow and two more are excited when the winds stop blowing. From the analysis that leads to Eqs. (3.80) and (3.81) it follows that there is an eastward current, and a deepening of the thermocline, for a time $T + L/c$ at a point east of the forced region. From measurements in the eastern side of the basin it is impossible to distinguish between winds that persist for a long time over a small region and winds that persist for a short time over a large region. The oceanic response depends on both the zonal extent of the forced region and the length of time for which the winds blow.

The remote response to winds with a complex structure can be calculated as follows. Expand the forcing function and the dependent variables as a series of Parabolic Cylinder Functions $D_n(y)$ after the introduction of new variables

$$q = u + g'\eta/c = \sum q_n(x, t) D_n(y)$$

$$r = -u + g'\eta/c = \sum r_n(x, t) D_n(y)$$

Equations for q_n , r_n , and v_n can readily be derived by exploiting the orthogonality of the Cylinder Functions. The equation for q_0 is

$$\frac{\partial q_0}{\partial t} + c \frac{\partial q_0}{\partial x} = X_0(x, t) \quad (3.82)$$

where X_0 is the projection of the zonal windstress onto a Gaussian (the Cylinder Function D_0). Equation (3.82) describes the Kelvin waves excited by the wind and has the solution

$$q_0(x, t) = \int_{-\infty}^t X_0[x + c(t' - t), t'] dt' \quad (3.83)$$

For winds that are described by a Gaussian in longitude and time,

$$X = \exp\left[-(2x/L)^2 - (2t/T)^2\right] \quad (3.84)$$

the solution to (3.82) is

$$q = \frac{1}{4} \left[1 + \operatorname{erf} \left(\frac{2\epsilon x + 2ct/\epsilon}{(L^2 + c^2 T^2)^{1/2}} \right) \right] \exp \left(\frac{-4(x - ct)^2}{L^2 + c^2 T^2} \right)$$

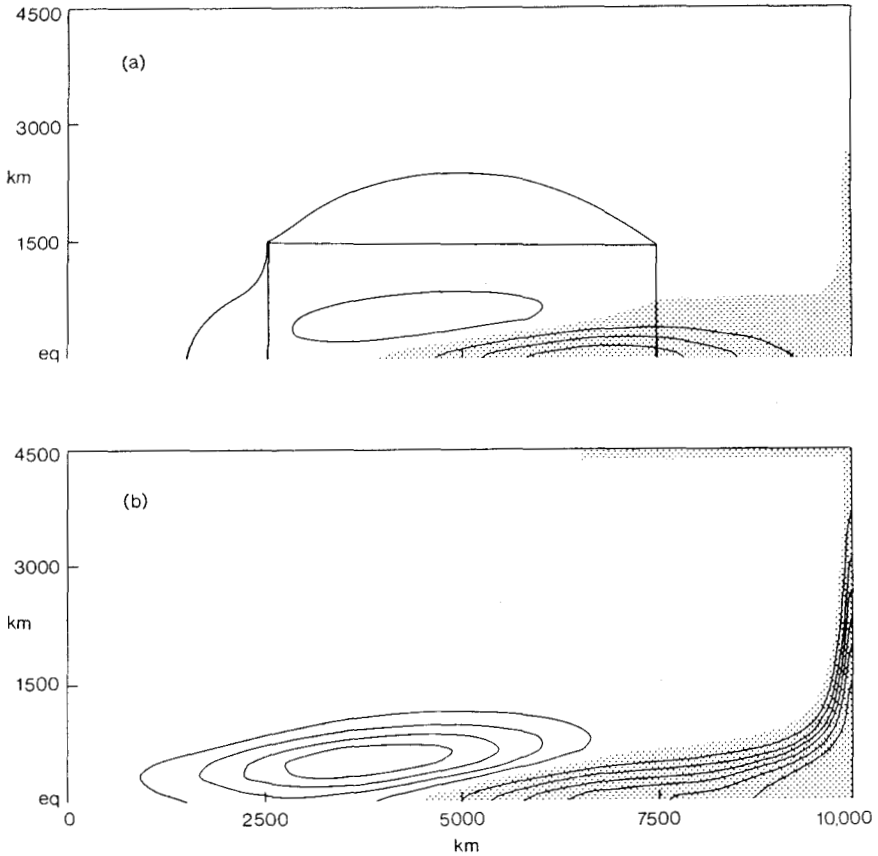


Figure 3.20. Changes in the depth of the thermocline in response to a patch of easterly winds with the zonal and latitudinal structure shown in (a). The maximum value of the windstress is 0.5 dyne/cm^2 . The instantaneous pictures show conditions after (a) 1 month, (b) 3 months, (c) 13 months, and (d) 60 months. Shaded regions indicate an elevation of the thermocline. The contour interval for curves that show departures from the mean depth of the thermocline is 10 m. [From McCreary and Anderson (1984).] (*Figure continues.*)

where $\varepsilon = cT/L$. Far to the east of the forced region the response is an eastward-traveling Gaussian pulse. At a fixed point it lasts a time $(T^2 + L^2/c^2)^{1/2}$. Fig. 3.21 shows a pulse, generated in the western Pacific, that traveled eastward nondispersively for several thousand kilometers along the equator.

The oceanic response is complicated if the areal extent of the forcing function gradually expands. This happened in 1982 when eastward winds

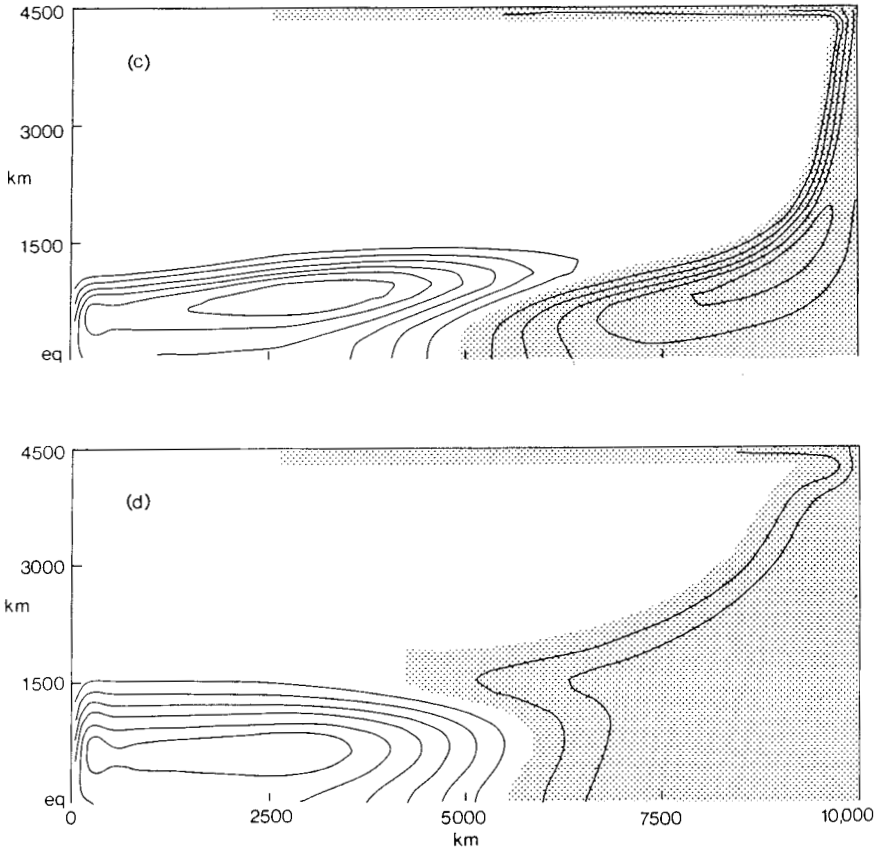


Figure 3.20 (Continued)

slowly penetrated farther and farther eastward in the tropical Pacific. Tang and Weisberg (1984) show that the response to a patch of westerly winds increases in amplitude if the patch moves eastward instead of remaining stationary. If the patch moves at the speed of a Kelvin wave then the response grows linearly with time. The eastward expansion of westerly winds during El Niño of 1982–1983 contributed to its large amplitude. In the tropical Atlantic the seasonal intensification of the southeast trades starts in the east and progresses westward. Rossby waves can then be forced resonantly (Weisberg and Tang, 1983, 1985; McCreary and Lukas, 1986).

Figure 3.20 depicts the oceanic response to eastward winds over a band of meridians in the middle of the basin. At first the winds deepen the thermocline to the east of the forced region but elevate it to the west. The

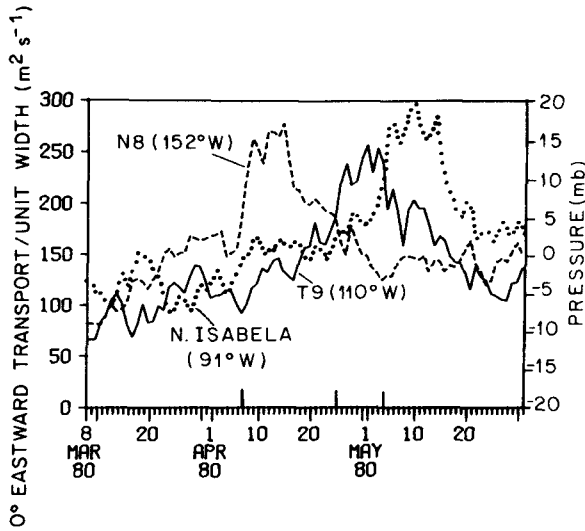


Figure 3.21. Eastward transport per unit width (essentially the average zonal current over the depth range 0 to 250 m) on the equator at 152°W and 110°W and sea level at Isabela Island in the Galápagos. A pulse progresses eastward. Its leading edge reaches 152°W on April 7, 110°W on April 25, and Isabela on May 3. [From Knox and Halpern (1982).]

elevation propagates westward as Rossby waves and reflects off the western coast an equatorial Kelvin wave that elevates the thermocline as it propagates eastward. In due course this elevation cancels the initial deepening of the thermocline in the forced region. This feature of the oceanic response is of enormous importance in some coupled ocean–atmosphere models of the Southern Oscillation (Chapter 6).

3.8 The Effects of Dissipation

In the absence of any mixing processes, steady, spatially uniform, zonal winds maintain a zonal pressure gradient but do not drive any currents (Eq. (3.10)). This property of linear inviscid models can disappear if nonlinear or dissipative processes are taken into account. In the shallow-water equations (3.1), include Rayleigh damping represented by a coefficient a and Newtonian cooling represented by a coefficient b :

$$\begin{aligned}
 u_t - \beta y v + g' \eta_x &= -a u + \tau^x / H \\
 v_t + \beta y u + g' \eta_y &= -a v + \tau^y / H \\
 g' \eta_t + c^2 (u_x + v_y) &= -b \eta
 \end{aligned}
 \tag{3.85}$$

If $b = 0$ and if a steady state is assumed so that a stream function ψ can be introduced, then

$$a\nabla^2\psi - \beta\psi_x = \text{curl}_z(\tau/H) \quad (3.86)$$

This equation implies that a wind with a curl that is zero does not maintain steady currents. The state of no motion that characterizes linear, inviscid models can persist even in the presence of Rayleigh damping. It is not the mixing of momentum but the mixing of heat that permits spatially uniform winds to drive steady currents. This is true for a bounded ocean. In a zonally unbounded ocean, spatially uniform zonal winds drive a steady equatorial jet (Yamagata and Philander, 1985):

$$\begin{aligned} u &= \frac{\tau^x}{aH}(1 - \xi Q) \\ v &= -\left(\frac{a}{b}\right)^{1/4} \frac{\tau^x}{H} (\beta c)^{-1/2} Q \\ \eta &= -(ab)^{1/2} \tau^x \frac{1}{c} Q_\xi \end{aligned} \quad (3.87)$$

where

$$\xi = y/\lambda' \quad \text{and} \quad \lambda' = (agh/b\beta^2)^{1/4}$$

This jet is a steady version of the one in Section 3.3 so that its structure—the function Q —is that shown in Fig. 3.4. Note the change in the latitudinal scale, the radius of deformation. It decreases as a approaches zero so that the jet becomes very narrow.

If north–south walls are present then the waves that are excited at the coast and that effect the oceanic adjustment attenuate as they propagate away from the coast. In the case of the Kelvin wave (McCreary, 1981b),

$$u = D_0(\xi) \exp[-(ab)^{1/2} x/c] \quad (3.88)$$

where D_0 is a Gaussian. If $a = b = 0$ then the steady solution in the presence of north–south walls is a state of no motion in which a zonal pressure gradient balances the spatially uniform wind. If $a \neq 0$, $b = 0$ then the steady state is again one of no motion. However, if $a = 0$, $b \neq 0$ then

$$\begin{aligned} u &= -\frac{2c^2\tau^x}{by^4\beta^2H} + \left(\frac{c^2}{b\beta y^2} + L - x\right) \exp(\beta by^2(x - L)/c^2) \\ v &= -\frac{\tau^x}{\beta Hy} [1 - \exp(\beta by^2(x - L)/c^2)] \\ \eta &= -\frac{\tau^x}{b\beta y^2} [1 - \exp(\beta by^2(x - L)/c^2)] \end{aligned} \quad (3.89)$$

The waves attenuate as they propagate across the basin and the pressure gradient they establish is too weak to balance the wind. At the equator the flow is singular unless the mixing of momentum is taken into account. In other words, nonzero but finite-amplitude steady currents depend on the mixing of both heat and momentum. The steady equatorial currents described by this model are generally unrealistic because nonlinearities, discussed in the next chapter, are important.

3.9 The Effects of Mean Currents

The ratio of the speed of waves to that of mean currents is a measure of the influence currents have on waves. The equatorial Kelvin wave, which travels at 140 cm/sec, is faster than the observed equatorial currents and is least affected by the currents. Rossby waves, on the other hand, have a maximum speed of 50 cm/sec, which is less than the speed of the eastward equatorial jet in Fig. 3.1, and which is barely comparable to the speed of the North Equatorial Countercurrent. A simple model with which to study how these currents affect the waves assumes that the mean flow $U(y)$ depends on latitude only and is in geostrophic balance so that the thermocline depth $H(y)$ is given by

$$\beta y U + g' H_y = 0$$

Linear waves in the presence of the mean flow satisfy the equations

$$\begin{aligned} u_t + U u_x - (f - U_y) v + g' \eta_x &= 0 \\ v_t + U v_x + f u + g' \eta_y &= 0 \\ \eta_t + U \eta_x + (H u)_x + (H v)_y &= 0 \end{aligned} \quad (3.90)$$

Let $1/\sigma$ denote the time scale of the motion, L a zonal scale, and \bar{U} a zonal velocity scale, then the assumptions $\sigma \ll f$ and $\bar{U}/fL \ll 1$, neither of which is valid near the equator, permit derivation of the vorticity equation

$$\frac{D}{Dt} \left[\eta_{xx} + R^{-2} (R^2 \eta_y)_y - R^{-2} \eta \right] + B \eta_x = 0 \quad (3.91)$$

where

$$\frac{D}{Dt} = \frac{\partial}{\partial t} + U \frac{\partial}{\partial x}$$

The effective β is

$$B = f Q_y / Q$$

and the effective radius of deformation is R :

$$R^2 = g'/Qf$$

The potential vorticity is

$$Q = (f - U_y)/H(y)$$

If the quasi-geostrophic approximations are adopted then the radius of deformation is the constant $\lambda = (c/f)^{1/2}$ and Eq. (3.91) simplifies to

$$\frac{D}{Dt} \left[\nabla^2 \psi - \frac{1}{\lambda^2} \psi \right] + \left[\beta + \frac{U}{\lambda^2} - U_{yy} \right] \psi_x = 0 \quad (3.92)$$

From this equation there follows a dispersion relation for plane waves of the form $\exp[i(kx + ny - \sigma t)]$, where the latitudinal scale $1/n$ is much smaller than that of the mean current:

$$\begin{aligned} \sigma &= kU - k \frac{\beta - U_{yy} + (U/\lambda^2)}{k^2 + n^2 + (1/\lambda^2)} \\ &= \frac{Uk(k^2 + n^2) - \beta k + kU_{yy}}{k^2 + n^2 + (1/\lambda^2)} \end{aligned} \quad (3.93)$$

Long waves ($k^2, n^2 \ll 1/\lambda^2$ and $k < (U/\beta)^{1/2}$) have the dispersion relation

$$\sigma = -k\lambda^2(\beta - U_{yy})$$

and are unaffected by a mean current without shear. Contrary to expectations, the frequency σ is not equal to that of a Rossby wave in the absence of mean flow, Doppler shifted by kU . The Doppler shift is canceled by the effect of the mean thermocline slope on the vorticity gradient. This shows that the ratio of the speed of the wave to that of the current is not a reliable indicator of the effect of currents on waves.

The quasi-geostrophic equations assume a constant value for the Coriolis parameter and its derivative. To explore how the latitudinal variations of the Coriolis parameter, as well as the presence of mean currents, affect the propagation of Rossby wave packets, it is necessary to revert to Eq. (3.91). If the nonconstant coefficients of this equation are assumed to be slowly varying functions of latitude in comparison with the meridional scale $1/n$ of the waves, then the application of the WKB method leads to the dispersion relation (Chang, 1988; Chang and Philander, 1988)

$$\sigma = kU - Bk/(n^2 + k^2 + R^{-2})$$

where

$$B = (\beta - U_{yy} + U/R^2) \frac{f}{f - U_y}$$

This dispersion relation can be used to calculate ray paths for packets of waves with a fixed frequency σ and zonal wave number k provided the initial meridional wave number n is specified. As a simple example consider the case in which the shear of the mean flow is so small that $U_y \ll f$ and $U_{yy} \ll \beta$ so that

$$R^2 \sim g'H(y)/f^2(y)$$

and

$$B \sim \beta + U/R^2$$

If the long (zonal) wave approximation is made then

$$\sigma \sim -\beta k g'H(y)/f^2$$

Although the curvature of the mean flow may not modify the β effect, the slope of the thermocline associated with the mean geostrophic current strongly influences Rossby wave propagation. The shallower the thermocline, the slower the waves. A westward current, and the associated equatorward shoaling of the thermocline, can cause the zonal speed of Rossby waves to decrease with decreasing latitude. (In the absence of mean currents this speed increases as the equator is approached.) Eastward mean currents, on the other hand, magnify the zonal speed of Rossby waves.

Realistic mean currents strongly affect ray paths as is evident from Fig. 3.22. Waves with a period of one year, and with the indicated wavelengths, are seen to have critical layers near 10°N and 3°N , where their phase speed equals that of the mean flow and where the mean current absorbs the waves. This absorption can prevent the waves from reaching certain regions. Figure 3.22 clearly shows that the waves from the Southern Hemisphere have difficulty penetrating farther north than approximately 3°N while those from the north cannot penetrate much farther south than 10°N . Westward currents such as the North Equatorial Current enhance the westward speed of Rossby waves but inhibit their meridional propagation. In Fig. 3.22, waves to the north of 10°N are therefore capable of crossing a basin as wide as the Pacific before they reach the critical layer near 10°N . (In the absence of mean currents—see Fig. 3.7—the waves have a far larger meridional group velocity.) This could explain why, in the measurements, waves to the north of 10°N appear to propagate across the Pacific without significant equatorward refraction (Pazan *et al.*, 1986).

The oceanic adjustment to a change in the winds is effected by waves described by Eq. (3.91). In the absence of mean currents there is an infinite set of discrete latitudinal modes. The fastest ones are equatorially trapped; slower ones propagate to higher latitudes. In the presence of mean currents the slower waves have critical layers and the set of waves that effects the

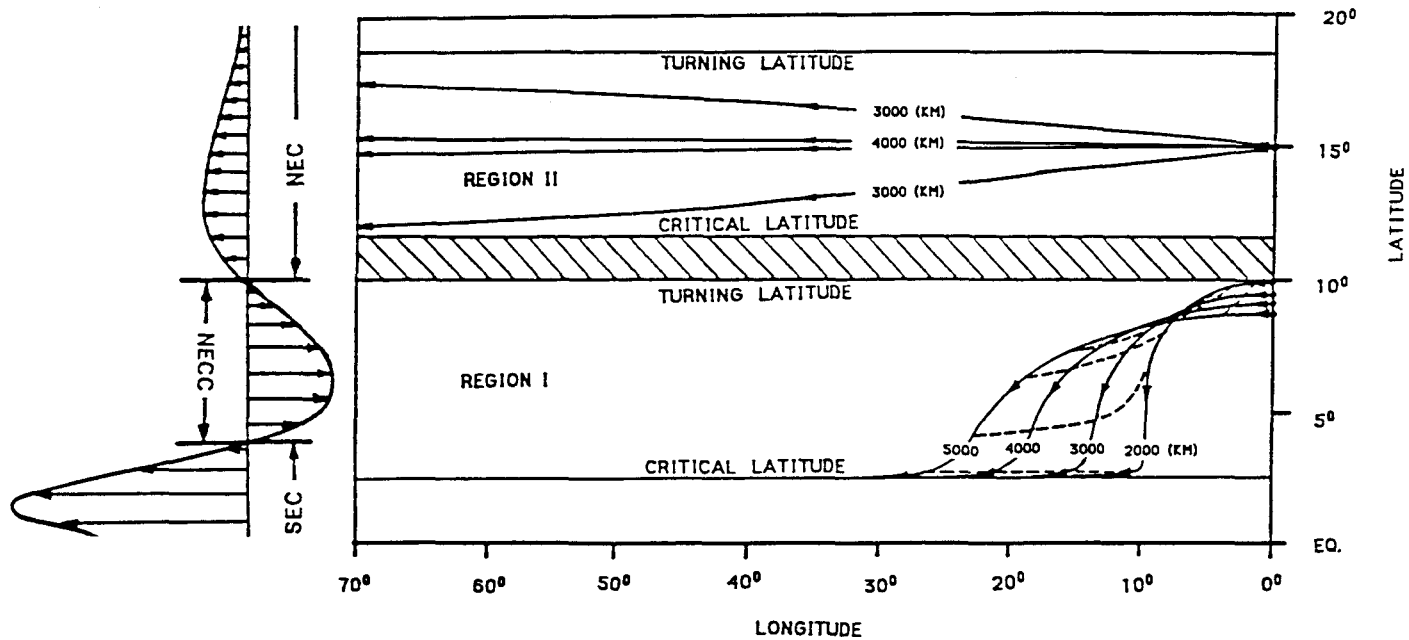


Figure 3.22. Ray paths of wave packets with a period of one year and with the indicated zonal wavelength in the presence of the realistic mean currents shown in the left-hand panel. The dashed lines are constant phase contours at intervals of 30 days. [From Chang and Philander (1988).]

adjustment falls into two groups. One group consists of a finite number of discrete latitudinal modes that are equatorially trapped and the other group consists of a continuum (not a discrete set) of modes each of which is bounded by either two critical layers or a critical layer and a turning latitude. The meridional structures of the equatorially trapped modes no longer correspond to the gravest Hermite functions but are affected by the mean currents and can be calculated by perturbation methods (McPhaden and Knox, 1979; Ripa and Marinone, 1983) or numerically (Philander, 1979a). This finite set of modes together with the continuum forms a complete set. Chang (1988) has developed a formalism that describes the oceanic response to wind variations in terms of these two groups of waves. The adjustment near the equator involves the modified equatorially trapped modes and is very similar to that described in Section 3.6. The adjustment far from the equator involves the continuum whose members all have critical layers. If the forcing function excites waves with small meridional group velocities—waves with long zonal wavelengths satisfy this condition—then critical layer absorption is unimportant and the waves, whose structure and speed depend on the mean flow, succeed in effecting an adjustment. This happens if the forcing function corresponds to an abrupt change in winds that are otherwise steady, or if the winds are periodic and have a low frequency. The waves have a significant meridional group velocity in the case of the annual and semiannual cycles. This means that critical layer absorption is important so that the waves fail to reach certain regions, which therefore respond strictly to local winds. In such regions, vertical movements of the thermocline are dictated by local Ekman suction and do not correspond to a Sverdrup balance. Figure 3.22 suggests that the neighborhood of 10°N is such a region, a result consistent with measurements (Meyers, 1980; Katz, 1987b). The same figure shows that eastward currents enhance meridional propagation and hence the speed with which waves reach critical layers. For this reason it is expected that the western part of the North Equatorial Countercurrent will not have a Sverdrup balance. Measurements with which to check this result are unavailable at this time.

3.10 Instabilities

Currents can become unstable under certain conditions that permit small perturbations to amplify. The conditions necessary for stability can readily be determined for currents $U(y)$ that are zonal and that are a function of latitude only. Assume that these currents are in geostrophic balance so that perturbations to the flow are described by Eqs. (3.90). The current $U(y)$ is

stable to infinitesimal perturbations provided there exists a constant α such that (Ripa, 1983)

$$(\alpha - U)Q_y > 0 \quad (3.94a)$$

$$(\alpha - U)^2 < g'H(y) \quad (3.94b)$$

for all y , where $Q = (\beta y - U_y)/H(y)$ is the potential vorticity of the mean flow. A well-known special case of this general stability condition requires that the flow be nondivergent [$g' \rightarrow \infty$, $Q_y \rightarrow (\beta - U_{yy})/H$] so that condition (3.94b) is trivially satisfied. By choosing α to be outside the range of U , stability is then assured provided the potential vorticity gradient Q_y does not change sign.

Stability analyses indicate that eastward equatorial jets with widths similar to those of the Equatorial Undercurrent are unstable provided their speeds exceed 1.5 m/sec. (The jets are assumed to be steady.) This sinuous mode of instability causes the jet to have eastward-propagating meanders about the equator. Its period is close to a month and its wavelength is of the order of 1000 km (Philander, 1976). Such instabilities have been excited in numerical models of the oceanic circulation but have not yet been observed in the ocean because eastward equatorial jets seldom attain a sufficiently high speed for a prolonged period. (There is also a varicose mode of instability in which perturbations remain symmetrical about the equator but the growth rate of this mode is slower than that of the sinuous mode.)

Instabilities associated with the shear of the westward South Equatorial Current and the eastward North Equatorial Countercurrent are common in the Pacific and Atlantic Oceans and are described in Section 2.7. Calculations for the observed currents indicate that they are stable in March and April, when both the South Equatorial Current and the North Equatorial Countercurrent are weak. They are unstable during the rest of the year, primarily because of the westward jet just north of the equator. Figure 3.23 shows a dispersion diagram for waves caused by instabilities of the surface currents in Fig. 2.1. The period, structure, and wavelength of the most unstable wave are in reasonable agreement with the measurements. This analysis, based on Eqs. (3.90), simplifies the vertical structure of the flow considerably. Calculations with a model that has realistic vertical structure indicate that the instabilities draw on both the kinetic and the potential energy⁶ of the mean flow (Cox, 1980). Realistic General Circulation Models include an additional complication—zonal and temporal inhomogeneities of the mean flow. The simulations, shown in Fig. 2.24, are strikingly similar to sea surface temperature patterns in satellite photographs. Further analyses of the results from the models are necessary.

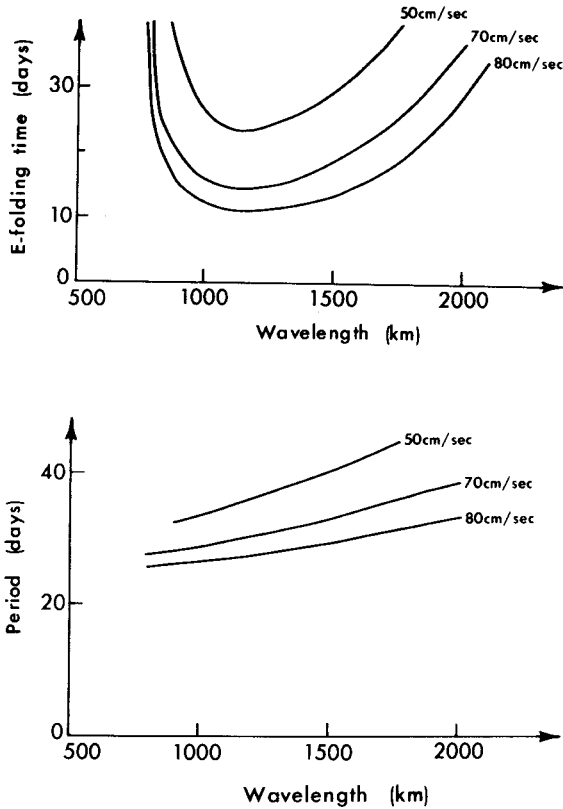


Figure 3.23. The e -folding time and period as a function of wavelength of waves associated with instabilities of the surface currents shown in Fig. 2.1. The curves correspond to different amplitudes of the zonal current. The shape of the profile $U(y)$ is the same for all the calculations, but the amplitude, which is taken to be the maximum speed of the South Equatorial Current, is varied. [From Philander (1978b).]

3.11 Discussion

The shallow-water model is one of the most powerful tools available to oceanographers. It provides answers to the questions raised by the measurements depicted in Figs. 3.1 and 3.2, but the measurements, which motivated the analyses presented here, prove too meager for a rigorous test of the theoretical results. Because the data are sparse, different interpretations of the measurements are possible. If the onset of the westerly winds over the Indian Ocean is taken to be instantaneous, then Kelvin and Rossby wave fronts are excited at the western and eastern extremes of the forced region,

respectively. The Kelvin wave establishes a zonal pressure gradient and can be invoked to explain why, in Fig. 3.1, the acceleration of the jet stops a few weeks after the sudden onset of the winds. The Rossby wave could have caused the subsequent deceleration of the jet. Figure 3.2 seems to confirm the presence of the Rossby wave but there are no measurements to confirm that a Kelvin wave actually arrested the initial acceleration of the jet. This opens the door to a different interpretation of the data provided it is taken into account that the wind changes are not instantaneous but occur over a period of weeks. This is far longer than the few days it takes a Kelvin wave to propagate from the western extreme of the forced region to Gan, where the measurements in Fig. 3.1 were made. (The westerly winds do not extend far west of Gan.) A zonal pressure gradient to balance the wind is therefore established within a matter of days. Hence the high correlation between the intensifying winds and the accelerating jet in Fig. 3.1 can be interpreted as an equilibrium response. The wind at each moment is balanced by a pressure force; the acceleration of the jet stops when the wind becomes steady; and the jet decelerates several weeks later when the eastward winds relax. However, if the relaxation is too sudden then the westward pressure force that the winds had maintained is left unbalanced and it decelerates the jet. This cannot be the entire story because Fig. 3.2 suggests that a Rossby wave played a role. A unique interpretation of the data in Fig. 3.1 clearly requires more measurements.

The shallow-water model is useful not only for studying idealized situations but also for simulating certain aspects of the oceanic response to the observed winds. The model is reasonably good at reproducing seasonal and interannual variations in the depth of the thermocline (Busalacchi and O'Brien, 1980, 1981; Busalacchi *et al.*, 1983). In certain parts of the ocean, the eastern tropical Pacific for example, there is a high correlation between sea surface temperature and thermocline depth variations so that the shallow-water model provides some information about sea surface temperatures. It is possible to go a step further by introducing thermodynamics in a simplified manner, so that sea surface temperature is an explicit variable, while retaining the one-layer formalism for dynamical purposes. An example of an equation for the temperature T of the upper ocean, from Anderson and McCreary (1985), is

$$(\eta T)_t + (u\eta T)_x + (v\eta T)_y = Q/\rho c_p + wT' - \bar{w}T \quad (3.95)$$

where T' is the specified constant temperature of the deep ocean, \bar{w} is a specified vertical velocity component that brings cold, deep water into the upper ocean, and w is an entrainment velocity given by

$$\eta(T - T')w = 2r - \eta Q/\rho c_p$$

where Q is the prescribed heat flux across the ocean surface and r is a specified rate of potential energy increase due to mechanical stirring by the wind. Schopf and Cane (1983) have a somewhat more elaborate procedure for calculating the temperature of the upper ocean. These simple models have proved valuable in studies of the interactions between the ocean and atmosphere (Chapter 6). They provide reasonable descriptions of sea surface temperature variations in response to certain windstress patterns but, because of the various approximations that are made, are sometimes unrealistic. To improve on these models it is necessary to take into account the continuous stratification of the ocean. The next chapter examines this subject.

Notes

1. Equations (3.1) in a spherical coordinate system, and with the appropriate forcing function, are Laplace's Tidal Equations. The Cartesian coordinate system of Section 3.2, known as the equatorial β -plane coordinates system, is an approximation to spherical coordinates and is accurate provided motion in a thin shell on a large sphere is confined to the tropics. Gill (1982) and Pedlosky (1987) derive these equations formally and state the approximations explicitly.

2. Matsuno (1966) provided the first consistent description of the properties of equatorially trapped waves in a shallow-water ocean. Lindzen (1967) first discussed their vertical propagation (Section 4.4). Some oceanographers refer to Rossby-gravity modes as Yanai waves, presumably after Professor Yanai, whose analysis of meteorological data revealed the presence of this mode in the atmosphere (Yanai and Maruyama, 1966). If these oceanographers were consistent they would refer to equatorial Kelvin waves as Wallace-Kousky (1968) modes.

3. The first few Hermite polynomials are

$$\begin{aligned} H_0 &= 1, & H_1 &= 2\xi \\ H_2 &= 4\xi^2 - 2, & H_3 &= 8\xi^3 - 12\xi \\ H_4 &= 16\xi^4 - 48\xi^2 + 12, & H_5 &= 32\xi^5 - 160\xi^3 + 120\xi \end{aligned}$$

Note that

$$\begin{aligned} \frac{dH_n}{d\xi} &= 2nH_{n-1} \\ \xi H_n &= nH_{n-1} + 0.5H_{n+1} \end{aligned}$$

4. The nonlinear interactions between various equatorial waves have been studied by Ripa (1982), Boyd (1980a and b), and others. One goal of these efforts is to explain the continuous spectrum of relatively high-frequency fluctuations in the ocean. In regions far from the equator where the fluctuations correspond to inertia-gravity waves, nonlinear interactions redistribute energy so that the spectrum, between the Brunt-Väisälä frequency and the inertia frequency, has a universal shape known as the Garrett and Munk (1979) spectrum. Close to the equator the fluctuations below the thermocline correspond to equatorially trapped waves but the spectrum is apparently not a universal one (Eriksen, 1981, 1985).

5. The seminal paper on oceanic adjustment is Lighthill's (1969) study of the generation of the Somali Current from a state of rest. The role of the equatorial Kelvin wave, which Lighthill overlooked, was pointed out by D. W. Moore and by Gill (1975), who investigated the generation of the Equatorial Undercurrent, and by McCreary (1976) and Hurlburt *et al.* (1976), who investigated the oceanic response to the relaxation of the trades during El Niño. The elliptically written series of papers by Cane and Sarachik (1976, 1977, 1979, 1981, 1983a) is a valuable and exhaustive study of the adjustment of a shallow-water ocean to various windstress patterns.

6. Baroclinic instability is not possible in a shallow-water model. In a two-layer system, currents with a given vertical shear become baroclinically more stable as their mean latitude decreases until, near the equator, there is no baroclinic instability. This is an artifact of the two-layer model. In a continuously stratified model the vertical scale of the baroclinically unstable waves decreases with decreasing latitude—it is zero at the equator—so that a two-layer model fails to resolve the waves near the equator (Held, 1978). Baroclinic instability near the equator has received little attention.